

This dissertation has been 63-7273
microfilmed exactly as received

SHIPPY, David James, 1931-
ELECTRICAL ANALOG OF THE POTENTIAL
DISTRIBUTION IN TWO-DIMENSIONAL UNSTEADY-
FLOW FIELDS.

Iowa State University of Science and Technology
Ph.D., 1963
Engineering, electrical

University Microfilms, Inc., Ann Arbor, Michigan

**ELECTRICAL ANALOG OF THE POTENTIAL DISTRIBUTION
IN TWO-DIMENSIONAL UNSTEADY-FLOW FIELDS**

by

David James Shippy

**A Dissertation Submitted to the
Graduate Faculty in Partial Fulfillment of
The Requirements for the Degree of
DOCTOR OF PHILOSOPHY**

Major Subject: Theoretical and Applied Mechanics

Approved:

Signature was redacted for privacy.

In Charge of Major Work

Signature was redacted for privacy.

Head of Major Department

Signature was redacted for privacy.

Dean of Graduate College

**Iowa State University
Of Science and Technology
Ames, Iowa**

1963

TABLE OF CONTENTS

	Page
INTRODUCTION	1
ESTABLISHMENT OF AN ANALOGY	3
SYNTHESIZING AN ANALOG	6
MATERIALS AND APPARATUS	12
Preliminary Studies	12
Conductive-Paper Analog	14
Conductive-Paint Analog	18
Electrolytic Analog	20
METHOD OF PROCEDURE	22
Measurement of Parameters	22
Obtaining of Transients	23
RESULTS AND DISCUSSION	30
Conductive-Paper Analogs	30
Measurement of parameters	30
Establishment of the validity of the analogs	35
Determination of time scales	45
Solution of a typical problem	58
Conductive-Paint Analog	65
Electrolytic Analog	77
Suggestions for Future Study	83
SUMMARY AND CONCLUSIONS	85
LITERATURE CITED	88

	Page
ACKNOWLEDGMENTS	90
APPENDIX	91
Derivation of the Differential Equation for Electric Potential within a Two-Dimensional, Continuous-Medium, Resistance-Capacitance Analog	91
Check on the Validity of the Assumption that $\partial \underline{A}_1 / \partial t$ is Negligible with Respect to $\nabla \phi_1$	96
Check on the Validity of Assumption that $ \epsilon_1 \rho (J_{z1})_2 \ll \sigma_{23} $	97
Check on the Validity of the Assumption that Variations of ϕ_1 with z are Negligible with Respect to ϕ_1	101

INTRODUCTION

In the study of certain physical phenomena, it is sometimes convenient to utilize observations upon other phenomena which are physically dissimilar but are described by the same differential equation (7, Part 3). For example, the behavior of a given flow field may be predicted from measurements made upon another flow field of essentially different nature. A formal analogy is then said to exist between the two fields, the one upon which the measurements are taken being termed an analog.

Unsteady-flow fields (having time-varying potential distributions) which occur in hydrodynamics, heat transfer, and electrodynamics are analogous in the sense defined above. Because of the relative ease of making electrical measurements and obtaining parameters, it is often desirable to study fields of the other types by means of electrical analogs.

Several investigators, only a few of whom are referred to here (9), (10), have used electric circuits containing lumped parameters (discrete resistors and capacitors) to analyze unsteady heat flow. To achieve good accuracy with such circuits in analyzing thermal fields of very irregular shape, it is necessary to use large number of circuit components, involving much complexity and cost. It therefore seemed desirable to devise a geometrical electrical analog with continu-

ously-distributed parameters.

Although electrical analogs with continuously-distributed resistance have been described by a few investigators (3), (8), (12), these analogs involved lumped capacitance, thus retaining the disadvantages of lumped parameters.

In an earlier study (11), the author described the conceptual design of a geometrical analog utilizing both resistance and capacitance in continuously-distributed form. The term geometrical is used to indicate that the analog is geometrically similar to the prototype as contrasted with electric circuits. The objective of the present investigation has been to find suitable materials for analogs of such design and to determine the validity of these analogs.

ESTABLISHMENT OF AN ANALOGY

The basic equation for a three-dimensional unsteady-flow field without sources or sinks is

$$\frac{\partial}{\partial x}(K_1 \frac{\partial \phi}{\partial x}) + \frac{\partial}{\partial y}(K_1 \frac{\partial \phi}{\partial y}) + \frac{\partial}{\partial z}(K_1 \frac{\partial \phi}{\partial z}) = K_2 \frac{\partial \phi}{\partial t} \quad (1)$$

where: ϕ = field potential

x, y, z = position coordinates

t = time

K_1, K_2 = field parameters, possibly functions of x, y, z

In one dimension, this expression reduces to

$$\frac{\partial}{\partial x}(K_1 \frac{\partial \phi}{\partial x}) = K_2 \frac{\partial \phi}{\partial t} \quad (2)$$

If K_1 is independent of position, this equation becomes

$$\frac{\partial^2 \phi}{\partial x^2} = K \frac{\partial \phi}{\partial t} \quad (3)$$

where $K = \frac{K_2}{K_1}$ = combined field parameter.

It is convenient to express this equation in terms of dimensionless variables. If K is independent of position, dimensionless variables may be defined as follows:

$$\xi = \frac{x}{s} \quad (4)$$

$$\tau = \frac{t}{Ks^2} \quad (5)$$

$$\beta = \frac{\phi}{\phi_0} \quad (6)$$

where s is a characteristic length of the field configuration and ϕ_0 is a characteristic potential of the field.

In terms of these dimensionless variables, Eq. 3 becomes

$$\frac{\partial^2 \phi}{\partial \xi^2} = \frac{\partial \phi}{\partial \tau} \quad (7)$$

An example of such a flow field is found in the conduction of heat in a one-dimensional homogeneous solid medium, the potential taking the form of temperature. With such a thermal system,

$$K_1 = k$$

$$K_2 = \rho c$$

$$K = \frac{\rho c}{k}$$

where: k = thermal conductivity of the medium

ρ = density of the medium

c = specific heat of the medium.

Equation 7 may thus be considered to describe the conduction of heat across a slab bounded by parallel planes and of infinite extent. The conduction of heat along a uniform rod with an insulated lateral surface is also represented by this equation.

Another example of the general type of flow field described above is found in the flow of electricity in a one-dimensional homogeneous solid medium. With such an electrical system,

$$K_1 = \frac{1}{\bar{R}}$$

$$K_2 = \bar{C}$$

$$K = \bar{R}\bar{C}$$

where: \bar{R} = resistance per unit length

\bar{C} = capacitance per unit length.

Hence Eq. 7 may also be considered to describe the flow of electricity along an insulated cable with resistance and capacitance continuously distributed along its length.

It can be seen that a formal analogy exists between the thermal and the electrical systems described above. The electrical system might therefore be used as a model or analog of a corresponding thermal system to predict the behavior of the latter, particularly because of the convenience of making measurements upon electrical systems.

SYNTHESIZING AN ANALOG

Obviously an electric cable would not be a very practical model for one-dimensional heat flow. However, such a cable may be represented approximately by the equivalent circuit shown in Fig. 1, the number of sections determined by the desired accuracy and the dimensions and properties of the body to be investigated (4, p. 124). The symbols R and C represent resistors and capacitors, respectively.

The usefulness of such an analog is limited, but may be increased by extending the analog to two dimensions. Such an extension of the above-mentioned circuit is illustrated by the circuit of Fig. 2. Although circuits of this kind have been used extensively by many investigators, there is inherent within them a limitation which restricts their usability. Specifically, if the thermal field to be investigated has irregular boundaries, the number of components required for good accuracy in an analog circuit could become prohibitive.

It therefore seemed desirable to devise a two-dimensional electrical analog in which the resistance and capacitance parameters would be continuously distributed rather than lumped as in the circuits described. In principle, such a result could be achieved by constructing a single extended capacitor, one plate of which would have a relatively high resistivity. There would thus be three layers in contact in

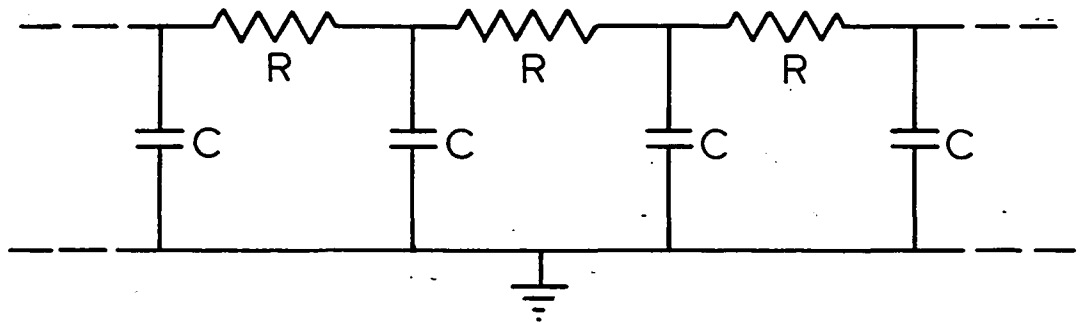


Fig. 1. Equivalent circuit for an inductionless electric cable

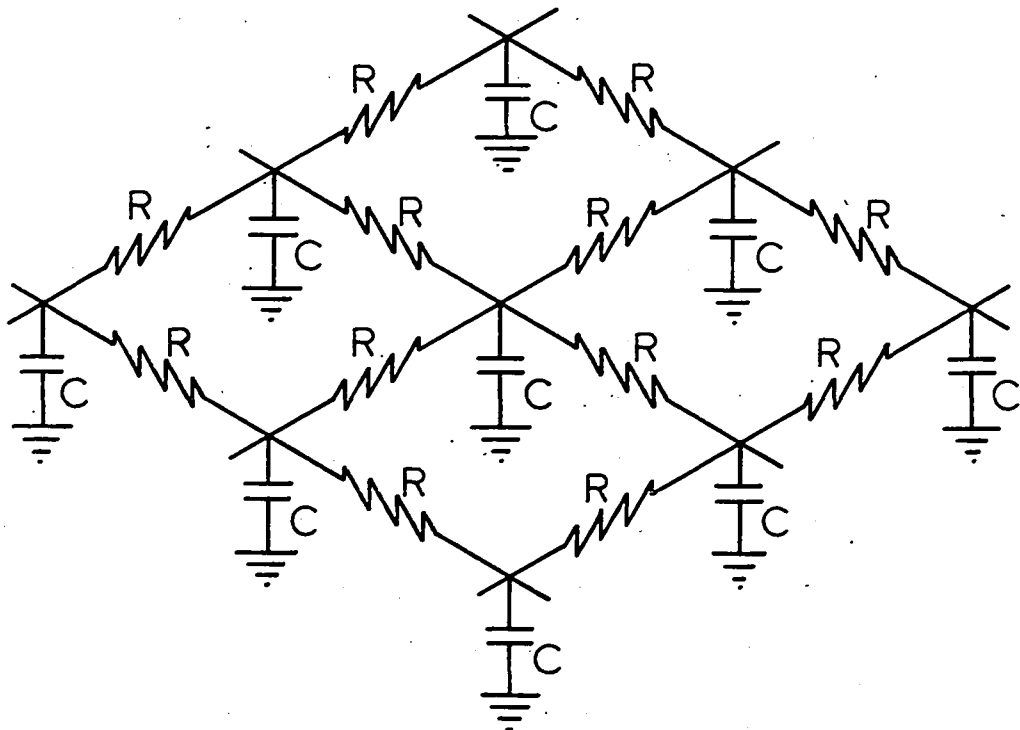


Fig. 2. Equivalent circuit for a two-dimensional flow field

the following order: a resistance layer; a dielectric layer; and a highly conductive ground layer. Conductive strips for the application of boundary conditions would be attached at appropriate locations along the boundary of the resistance layer. This basic concept is illustrated in Fig. 3.

Extended to two dimensions, Eq. 7 becomes

$$\frac{\partial^2 \theta}{\partial \xi^2} + \frac{\partial^2 \theta}{\partial \eta^2} = \frac{\partial \theta}{\partial \tau} \quad (8)$$

where $\xi = y/s$. The corresponding field coefficients now are

$$K_1 = \frac{1}{\bar{R}'}$$

$$K_2 = \bar{C}'$$

$$K = \bar{R}'\bar{C}'$$

where \bar{R}' is the resistance per unit length of a unit width of the resistance layer and \bar{C}' is the capacitance per unit area of the dielectric layer. In other words, \bar{R}' is the resistance from one edge to the opposite edge of a square region of a homogeneous medium of uniform thickness. This resistance is independent of the size of the square. For this reason, \bar{R}' is sometimes referred to as resistance per square, its units being ohms. In dimensionless polar coordinates, Eq. 8 is expressed as

$$\frac{\partial^2 \theta}{\partial \sigma^2} + \frac{1}{\sigma} \frac{\partial \theta}{\partial \sigma} + \frac{1}{\sigma^2} \frac{\partial^2 \theta}{\partial \alpha^2} = \frac{\partial \theta}{\partial \tau} \quad (9)$$

where: $\sigma = r/s$

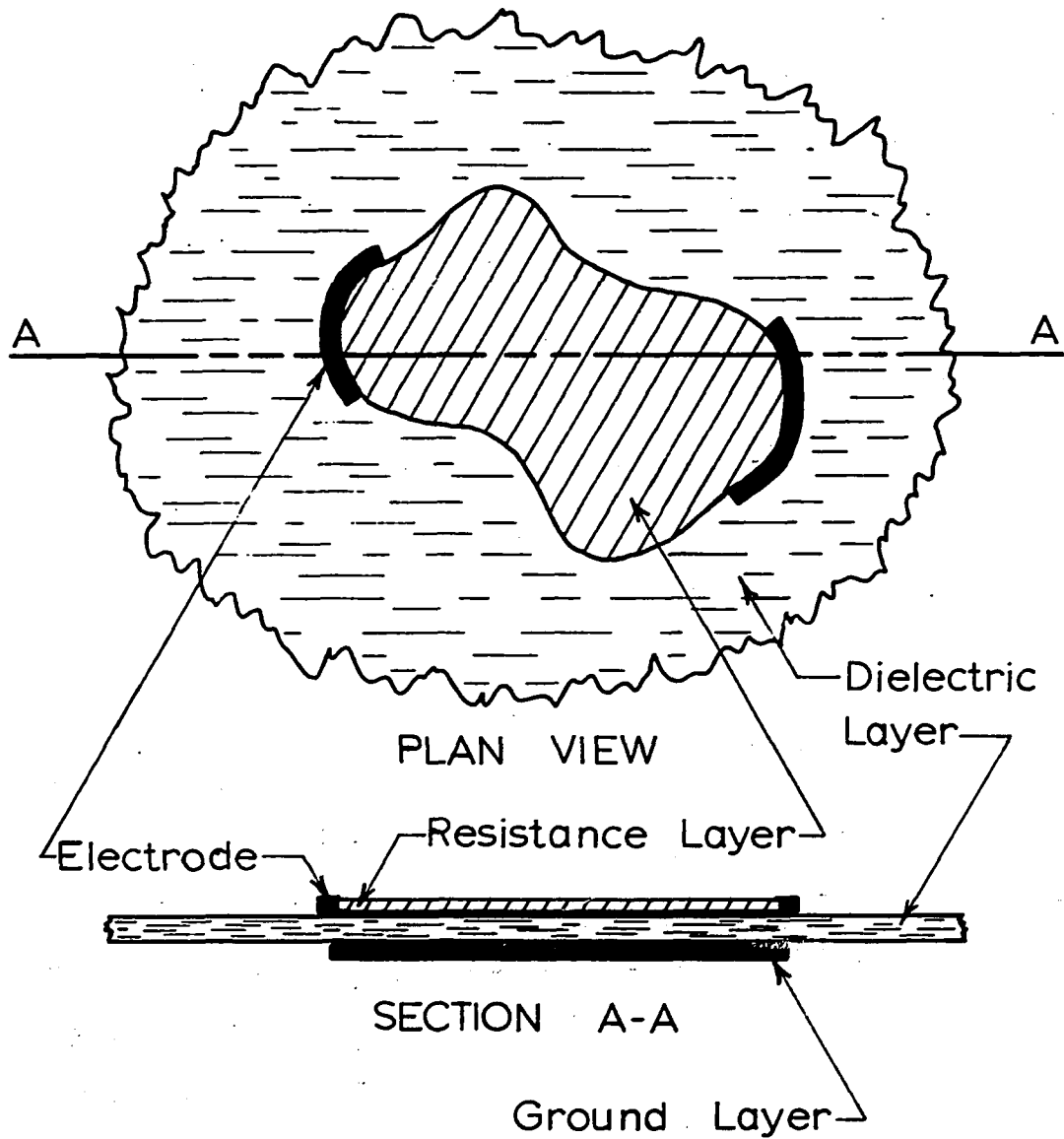


Fig. 3. Diagram of a continuous-medium analog for an arbitrary flow region

r = radial position coordinate (measured from the center of circular configurations)

α = angular position coordinate

The boundary conditions of the thermal-electrical analogy are as follows:

The boundary of the resistance layer must have the same shape as the boundary of the thermal flow region. Where portions of the thermal boundaries are insulated, the corresponding portions of the resistance-layer boundary must be insulated. Portions of the thermal boundary where the temperature is uniform but possibly varying with time are represented at the corresponding locations on the resistance-layer boundary by electrodes whose variations of voltage with time are controlled in accordance with the corresponding temperature variations.

A generalization of the flow problem to include the effects of leakage may be made. In the thermal system, the leakage would consist of convection and radiation between an exposed surface of a thin sheet of the thermal medium and its environment maintained at a constant temperature. In the electrical system, the leakage would consist of conduction through the dielectric layer, i.e., conduction between the resistance layer and the ground layer.

The general field equation for a system in which leakage

occurs is

$$\frac{\partial^2 \theta}{\partial \xi^2} + \frac{\partial^2 \theta}{\partial \eta^2} - H(\theta - \theta_e) = \frac{\partial \theta}{\partial \tau} \quad (10)$$

where H is the dimensionless leakage parameter and θ_e is the dimensionless potential of the environment (the voltage of the ground layer for the electrical system). In the thermal system,

$$H = \frac{hs^2}{k}$$

where h is the surface coefficient of heat transfer (heat/unit time/unit area/unit temperature difference between the medium and its environment). In the electrical system,

$$H = \bar{R}'\bar{G}'s^2$$

where \bar{G}' is the shunt conductance to ground per unit area of the dielectric layer.

It is to be noted that considerable use has been made of continuous-medium, two-dimensional electrical analogs (conductive paper, electrolytic tank, etc.) for the solution of steady-state problems. By the introduction of distributed capacitance as described in this thesis, such steady-state analogs are extended for the study of transient-flow problems.

MATERIALS AND APPARATUS

Preliminary Studies

The objective of the present research has been to develop and establish the validity of a two-dimensional electrical apparatus with uniformly distributed resistance and capacitance as an analog for unsteady flow fields.

It was necessary first to search for materials which, when combined in the three types of layers previously mentioned, would be suitable for the purposes of this study. The primary criteria used in the selection of materials were (a) the existence of a time constant (product of \bar{R}' and \bar{C}') sufficiently large to permit observation of transients and (b) the absence of leakage through the dielectric. This second requirement was relaxed in the case of analogs for flow with leakage. For simplicity, the analogs used in the experimental research were designed to have uniformly distributed resistance and capacitance.

The assumptions utilized in the first step were the following: (a) uniform distribution of resistance throughout the resistance layer; (b) uniform conductance through the dielectric layer (negligible in the case of no leakage); (c) uniformity of thickness and dielectric constant of the dielectric layer; (d) negligible resistance of the ground layer; (e)

negligible resistance of the boundary electrodes.

Among the materials tested for each of the three layers were the following:

<u>Resistance</u>	<u>Dielectric</u>	<u>Ground</u>
conductive paper	ordinary paper	aluminum foil
liquid electrolyte	aluminum oxide	aluminum plate
conductive paint	coats of lacquer	conductive paint
	coats of epoxy varnish	
	sheet plastic	

The lacquer was found to be apparently dissolved by a coat of conductive paint on its surface. Attempts to use the epoxy varnish on aluminum plate resulted in coats which were either too thick or nonuniform.

For systems displaying no leakage, the combination of conductive paper, sheet plastic, and low-resistance conductive paint was the most successful. The use of high-resistance conductive paint in place of the paper also indicated good potential. Liquid electrolyte used in conjunction with anodized aluminum foil showed the most promise for the case of leakage. (This latter combination is the same as that used in the manufacture of electrolytic capacitors.) These three types of analogs, hereafter referred to as paper, paint, and electrolytic, respectively, are discussed separately in the following sections.

Conductive-Paper Analog

It was necessary initially to provide some means of holding flat the plastic sheet which served as a dielectric layer. To provide for this, special frames in the shape of hollow rectangles were cut from a sheet of masonite. A rectangular sheet of "Saran Wrap" plastic (the dielectric layer) was fastened to the smooth surface of each frame by means of small pieces of cellophane tape. The plastic sheet was fastened first at the centers of the edges, then at the corners, and finally at several other positions along the edges. With this procedure, the plastic sheet could be stretched uniformly taut, thus eliminating wrinkles.

The ground layer, a coat of low resistance paint (Micro-Circuits Company SC12 Silver Paint), was brushed upon the exposed surface of the plastic sheet with the smooth side of the masonite down. A piece of aluminum foil, extending outside the masonite frame, was placed in contact with the paint while still wet. This piece of foil, secured to the masonite, permitted convenient access to the auxiliary electronic equipment.

The resistance layer for a given analog consisted of a sheet of "Teledeltos" carbon-impregnated paper. This sheet was placed in contact with the unpainted surface of the plastic sheet. One surface of the "Teledeltos" paper appears silver while the other appears black. In most cases, the

black side was placed in contact with plastic. Each sheet of paper was cut to the shape of the field to be investigated. Boundary electrodes for the application of potentials consisted of coats of silver paint at appropriate locations. Also, small spots of silver paint were coated at appropriate locations on the top surface of the paper for adequate electrical contact with the probe electrodes.

Preliminary investigation indicated that uniformity of contact between the paper and the plastic was necessary to provide uniform distribution of electrical parameters. This uniformity of contact seemed to be directly related to the uniformity of distribution of pressure between these two layers. After unsuccessful attempts to use such materials as modelling clay to distribute the pressure holding the layers together, it was decided that the use of a fluid (to eliminate shearing stresses) would be necessary.

For this reason, a sealed, shallow wooden box was constructed to serve as an air chamber. The top of the box consisted of a very thin rubber membrane to seal the box and to transmit the pressure inside the box. In use, the box served as a base upon which the plastic sheet and the paper sheet were laid. A piece of 1/4-inch tempered masonite with imbedded probe electrodes served as a retainer at the top, the entire assembly being clamped together with a plywood frame secured by carriage bolts and wing nuts at the four corners

of the assembly.

The probe electrodes were No. 4 x 1/2-inch brass machine screws which were screwed from the top into holes in the masonite so as to protrude slightly at the bottom surface. The screws were then sanded flush with the bottom surface. Adjustment of the screws for proper contact was conveniently made with a screwdriver. The holes for the screws were spaced at appropriate intervals in a square array over a ten-inch-square region.

Finally, the compressed air was supplied through a hole in the side of the air chamber. At low values, pressure was measured with a U-tube water manometer and at high values with a pressure gage. The pressure was regulated with a valve and a floating steel ball. Use of the steel ball facilitated the removal and reapplication of pressure in the air chamber during the changing of sheets of paper.

The entire pressure apparatus is illustrated by the exploded view of Fig. 4.

It should be pointed out that considerable reinforcement of the air chamber as it is described above was necessary when operating at pressures above 1 psi.

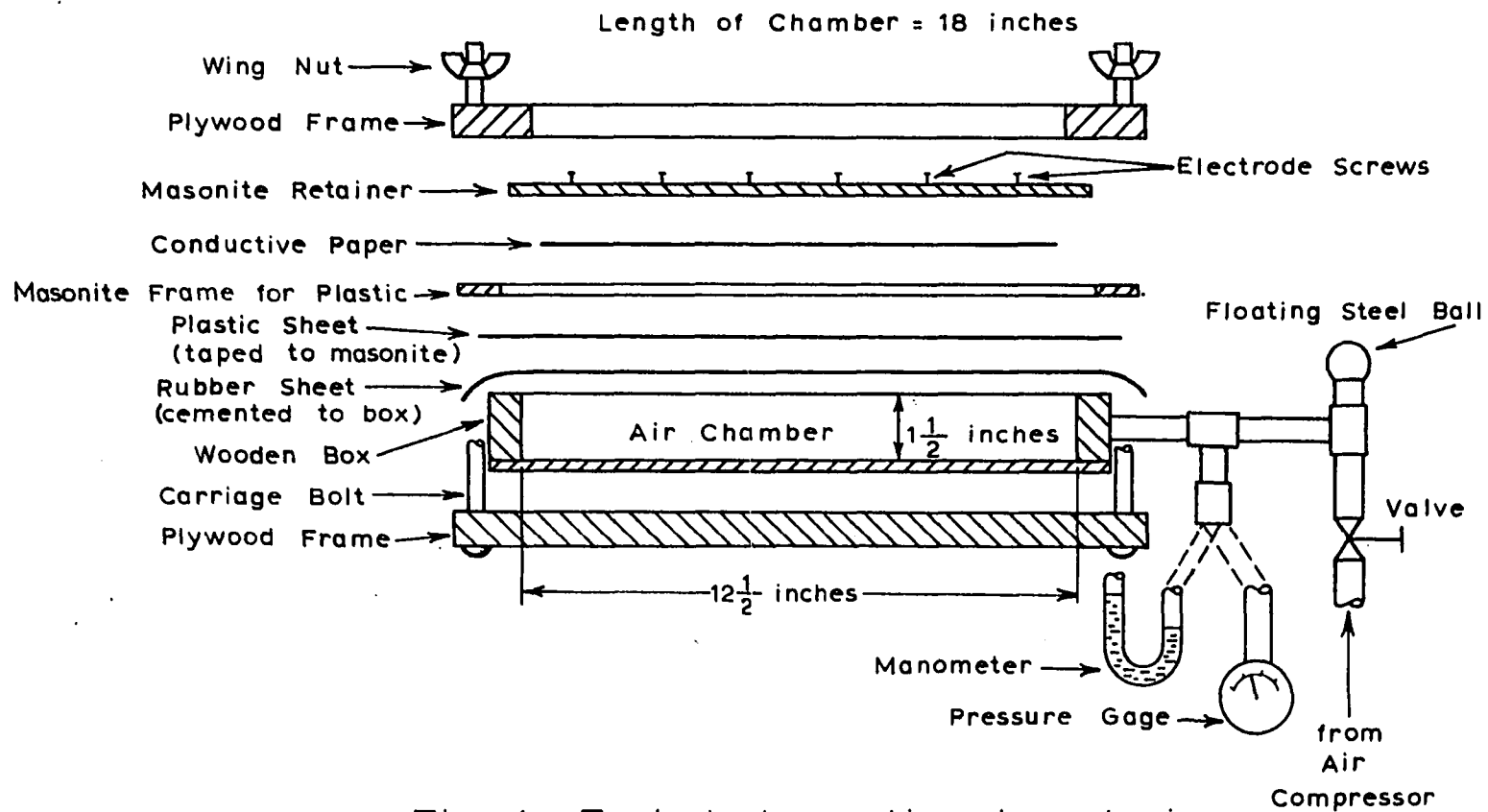


Fig. 4. Exploded sectional end view of pressure apparatus

Conductive-Paint Analog

As with the paper analogs, the first step in the construction of a paint analog was the fastening of a sheet of "Saran Wrap" plastic to the surface of a hollow rectangular masonite frame.

The resistance layer, a coat of electrically-conductive paint of relatively high resistance (Micro-Circuits Company R11 and sometimes R21 Resistance Paint), was brushed upon the exposed surface of the plastic with the smooth side of the masonite down. This surface was chosen so that the plastic sheet would lie flat against a supporting plane surface when a probe contacted the resistance layer. The boundary of the painted area was of course determined by the configuration desired. During this operation, considerable illumination from the opposite side of the plastic was provided to insure that the entire designated area was covered with paint.

Next, a strip of conductive paint of relatively low resistivity (Micro-Circuits Company S012 Silver Paint) was brushed upon the plastic along designated parts of the boundary of the previously painted region. This strip, slightly overlapping the resistance layer, formed the electrode (or electrodes) where the boundary conditions were applied. Pieces of aluminum foil were placed in contact with the paint while wet. These pieces of foil, secured to the masonite frame, permitted convenient access to the auxiliary equipment.

Finally, a coat of the low resistance paint (the ground layer) was brushed upon the opposite surface of the plastic sheet, covering the region described by the resistance layer. It might be noted here that an earlier design involved the taping of the plastic sheet to an aluminum plate which served also as the ground layer. The results obtained from these models were less satisfactory, apparently because of lack of intimate contact between the plastic and the aluminum. The capacitance was definitely not as great and probably not as uniform as with the accepted design.

The first analogs studied involved one-dimensional flow along narrow rectangular strips. Such regions were masked off with parallel strips of cellophane tape. When the resistance layer had dried, that part of the paint which overlapped the cellophane tape was merely scraped off with a razor blade. This procedure resulted in well defined lateral edges of the resistance layers. Silver paint electrodes bounded the ends of the resistance strips.

Another analog studied involved two-dimensional flow within a solid circle with an electrode along the entire circumference. A circular region of the plastic sheet was masked off with masking tape, which was removed after the resistance layer had dried. This permitted the application of the silver paint electrode.

Electrolytic Analog

The construction of electrolytic analogs begins with the preparation of the electrolyte. The composition of a suitable electrolyte and directions for its preparation were provided by a manufacturer of capacitors. This composition was as follows:

ethylene glycol	5 parts (by weight)
boric acid (powder)	5 parts
ammonium hydroxide (28-30% NH_3)	1 part

The boric acid and the ammonium hydroxide were obtained in reagent grade because a high purity of the electrolyte is essential for a proper interaction with the aluminum oxide, as indicated in the literature (5). Even small amounts of impurities can considerably increase the leakage through the dielectric layer. Impurities such as chlorides are especially critical.

The electrolyte is prepared by first mixing the components in the order listed above. As mixed, the water content of the electrolyte is quite high. When the mixture is boiled, the water gradually vaporizes, resulting in a corresponding increase in boiling temperature. This is accompanied by an increase in viscosity and electrical resistivity. This process can be reversed by the addition of distilled water. Thus the resistivity can be controlled by boiling and/or addition

of water and can be measured by the boiling temperature of the mixture. In this way, batches of electrolyte with the same characteristics can be produced.

In the present investigation, sheets of anodized aluminum foil were taped to a flat surface. (Rolls of anodized foil of various voltage ratings were made available by the capacitor manufacturer mentioned above.) One or two layers of facial tissue were then laid on the surface of the anodized foil. These served as a separator between the probe and the oxide coating to minimize the possibility of short circuits through the oxide. Next, the electrolyte was poured upon the tissue, which absorbed much of the electrolyte. Finally, boundary electrodes of sheet lead, chosen for its chemical inertness, were laid upon the tissue to be in intimate contact with the electrolyte at desired locations.

METHOD OF PROCEDURE

Measurement of Parameters

Once the materials for the analogs were selected and assembled, investigations were made to establish the validity of the analogs, the extent to which their behavior was as described by the equations presented earlier. This investigating involved the direct measurement of certain parameters and also the obtaining of analog voltage transients for some simple configurations.

One of the parameters evaluated by direct measurement was \bar{R}' (the resistance per square of the resistance layer) for the paper and the paint analogs. This was done by first measuring (with a volt-ohmmeter) the end-to-end resistances of several one-inch-wide rectangular strips of the resistance layer. (Silver paint electrodes were used at the ends of the strips.) The resistances per unit length of the various strips were then compared.

Similar measurements were made to determine the magnitude of \bar{C}' (the capacitance per unit area of the dielectric layer). For the paper analogs, this was accomplished by placing several equal-sized square pieces of conductive paper side by side in the pressure apparatus described earlier, thus forming small analog sections. The capacitance of each of these analog sections was then measured (with an impedance bridge)

at a given pressure. The capacitances per unit area of the various sections were compared. For the paint analogs, the determination of \bar{C}' was made solidly coating one surface of a plastic sheet with silver paint, coating the opposite surface with rectangular sections of silver paint, and measuring the capacitance of each section.

Another procedure for evaluating \bar{C}' of paint analogs involved coating with silver paint the exposed surface of the resistance layer of an already constructed analog. The capacitance between this layer of silver paint and the ground layer was measured.

An attempt was made to determine the leakage conductance through the dielectric layer of each conductive-paint analog, this conductance assumed to be negligible. This was done by measuring the resistance between a boundary electrode and the ground layer.

Obtaining of Transients

To check further the validity of the analogs, voltage transients were obtained from several analogs for which exact analytical solutions were available.

It was felt that the simplest type of disturbance to introduce into an analog would be a step change in voltage. This could of course be effected simply by the mechanical switching of a constant d. c. voltage in or out of the analog

circuit at the electrodes and the ground layer. In addition to the possibility of noise difficulties with such a procedure, the rate of repetition of the transient would be limited considerably. For these reasons, a square-wave generator was used to produce repeating step inputs. By proper adjustment of the sweep mechanism of the oscilloscope used to record the resulting transients, the repeated transients from paper analogs and paint analogs appeared as standing patterns on the oscilloscope screen. The magnitude of the voltage at various times could thus be read conveniently. Synchronization of the oscilloscope sweep by means of a signal from the generator was found to be desirable.

The time constants of the electrolytic analogs were quite large due to the large capacitance per unit area. This resulted in relatively slowly-varying transients, standing patterns therefore not appearing. It was thus desirable to photograph the oscilloscope traces of these transients.

The boundary conditions selected were such that the boundary electrodes of each analog were electrically connected to each other and to the ungrounded terminal of the generator. The ground layer was similarly connected to the grounded terminals of the generator and the oscilloscope. With the electrolytic analogs, it was necessary to bias the input to the analog to ensure that the flow of current through the leaky dielectric layer was always in the direction from the

ground layer to the resistance layer (the electrolyte). This biasing is required for the proper functioning of the device (5, Chap. 6). It was accomplished by the insertion of a battery between the ungrounded generator terminal and the analog boundary electrodes, the positive battery terminal being connected to the generator. Reversal of this polarity results in a marked increase in leakage conductance.

A probe held in contact with any given point on the resistance layer transmitted the varying voltage at that point to the input of the oscilloscope. A diagram of the basic circuit used in conjunction with the analogs is shown in Fig. 5.

The specific electronic equipment used in conjunction with the electrolytic analogs consisted of a Hewlett-Packard Model 202A Low Frequency Function Generator and a Hewlett-Packard Model 122A Cathode-Ray Oscilloscope. This equipment did not prove satisfactory, however, for the conductive-paint analogs.

One of the difficulties encountered when R21 "Medium-Resistance Paint" was used for the resistance layer (as with the circle having an electrode along its entire circumference) was a loading effect by the oscilloscope upon the analog, causing a departure of analog behavior from that described by Eq. 8. This loading effect amounted to the shunting of a current through the oscilloscope, comparable in magnitude to

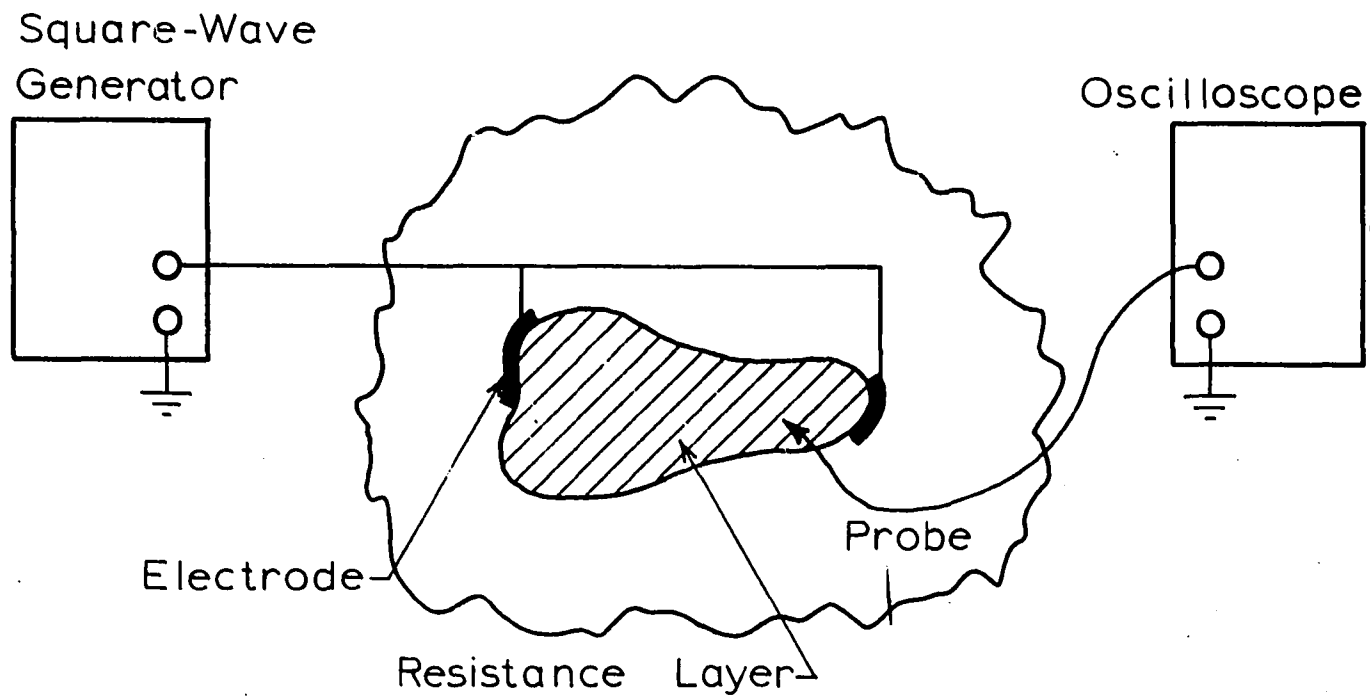


Fig. 5. Basic circuit used with the analogs

currents in the analog. Obviously this occurred because the impedance of the oscilloscope was not sufficiently higher than that of the analog. The use of a high resistance in series with the probe helped to alleviate this difficulty. This procedure resulted of course in a decrease in signal level to the oscilloscope.

Another approach to overcoming this loading difficulty was the use of Rll "Low-Resistance Paint" for the resistance layer. Here, as with the paper analogs, the analog impedance was small compared to the output impedance of the generator, and hence the analog now loaded the generator, resulting in a deteriorated square wave. Furthermore, with all analogs of appreciable area, the magnitude of the analog capacitance alone had a deleterious effect upon the output of the generator. The loading of the generator by the analog was finally minimized by the insertion of a compensating filter network between the generator and the analog as shown in Fig. 6.

A somewhat different difficulty was also encountered with the paint analogs and especially with the paper analogs. Because of the relatively low time constants of these analogs, it was necessary to "spread out" the associated oscilloscope traces (by using high sweep-writing rates) in order to determine accurately the shapes of the transients. This, however, accentuated the rise time of the generator, causing the output of the 202A generator to appear trapezoidal rather than square.

Square-Wave
Generator

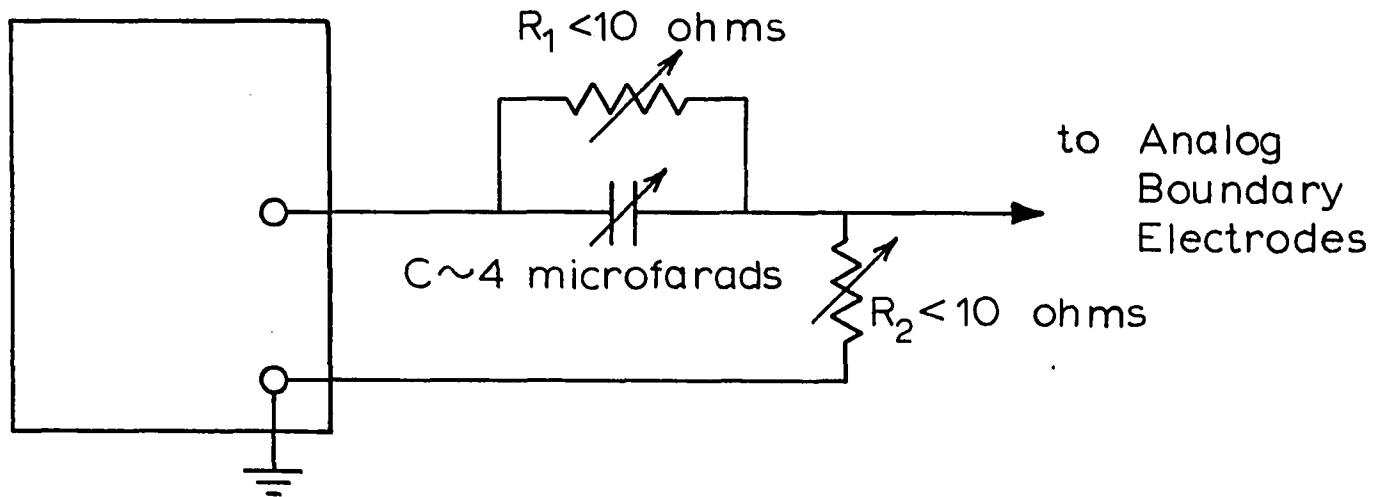


Fig. 6. Generator with external filter network
to compensate for the analog impedance

Furthermore, the response of the 304-H oscilloscope at the frequencies involved was such that it further impaired the appearance of the generator output signal. Hence, for obtaining transients from the paper analogs, a Hewlett-Packard Model 211-A Square-Wave Generator (75 ohm output, 0.02 microsecond rise time) and a Tektronix Type 543A Cathode-Ray Oscilloscope (with plug-in units of 0.01 microsecond rise time) were used. It should be noted that even with this generator of very short rise time at rated load impedance, the appearance of the square wave signal was unsatisfactory at the sweep rate required when the signal was applied to a ten-inch-square paper analog with an electrode around the entire perimeter. This was apparently due to the increased loading effect of the analog involved in this situation. Use of a higher resistance paper, thus increasing the time constant of the analog, would permit the use of lower frequencies and sweep rates, thereby alleviating the difficulty.

RESULTS AND DISCUSSION

Conductive-Paper Analogs

Measurement of parameters

As indicated previously, direct measurements of certain parameters were made to determine the validity of the assumptions made. The results of such measurements on paper analogs are presented in the present section.

To determine the uniformity of the resistance layers, a measurement was made of the end-to-end resistances of several short rectangular strips, one inch wide, cut from a roll of conductive paper. Half of these strips were originally oriented in the same direction, X, on the roll of paper, the other half in the perpendicular direction, Y. The results of these measurements are given in Table 1, along with the corresponding values of resistance per square, \bar{R}' . The average of the values of \bar{R}' was 1790 ohms, the average deviation from the mean being 70 ohms or about 4% of 1790 ohms. It should be noted that only about one half of the measured deviation was due to lack of homogeneity. As can be seen from Table 1, the other half was due to anisotropy.

To determine the uniformity of the capacitance, measurements were made of the capacitances of several 1.97-inch-square sections of paper analogs as indicated previously. The

Table 1. Resistances of one-inch strips of conductive paper

Original orientation of strip	Strip length (inches)	Total Resistance (ohms $\times 10^3$)	Resistance per square (ohms $\times 10^3$)
X	1.32	2.25	1.70
"	1.29	2.20	1.71
"	1.20	2.08	1.73
"	1.27	2.20	1.73
"	1.19	2.10	1.76
"	1.16	1.96	1.69
"	1.21	2.08	1.72
"	1.22	2.15	1.76
"	1.27	2.28	1.79
"	1.23	2.18	1.77
"	1.18	1.97	1.67
"	1.27	2.14	1.68
"	1.23	2.06	1.68
"	1.27	2.14	1.68
"	1.24	2.24	1.80
"	1.25	2.20	1.76
"	1.15	1.91	1.66
"	1.25	2.12	1.70
Y	1.14	2.18	1.91
"	1.12	2.10	1.87
"	1.06	1.97	1.86
"	1.17	2.12	1.81
"	1.22	2.24	1.84
"	1.29	2.40	1.86
"	1.15	2.16	1.88
"	1.08	2.04	1.89
"	1.06	1.97	1.86
"	1.12	2.04	1.82
"	1.28	2.42	1.89
"	1.34	2.48	1.85
"	1.14	2.12	1.86
"	1.18	2.24	1.90
"	1.15	2.14	1.86
"	1.16	2.14	1.84
"	1.19	2.18	1.83
"	1.22	2.22	1.82

results of measurements taken at two different pressures are presented in Table 2. The average capacitance per section at 11. inches of water was $1.73(10^{-9})$ farad, the average deviation from the mean being $0.07(10^{-9})$ farad or about 4% of $1.73(10^{-9})$ farad. At 2.5 psi, the average capacitance per section was $2.73(10^{-9})$ farad, the average deviation from the mean being $0.08(10^{-9})$ farad or about 3% of $2.73(10^{-9})$ farad. It thus appears that not only the magnitude of the capacitance but also its uniformity increases with pressure.

Further investigation into the effect of pressure upon the magnitude of the capacitance was made with a large paper analog. The results of this investigation are given in Table 3.

To check assumption (e), the end-to-end resistances of the boundary electrodes of several large paper analogs were measured. These analogs utilized 10.5-inch squares of conductive paper with 0.5-inch-wide electrodes painted along the entirety of two adjacent sides. The results of these measurements are given in Table 4.

A comparison of the resistance values of Table 4 to those of Table 1 (resistance per square of the conductive paper) would seem to indicate that assumption (e) is justified.

Table 2. Capacitances of 1.97-inch-square sections of
conductive-paper analogs (farads $\times 10^{-9}$)

Pressure = 11. inches of water	Pressure = 2.5 psi
1.87	2.69
1.81	2.67
1.83	2.76
1.73	2.52
1.71	2.57
1.90	2.67
1.75	2.69
1.81	2.70
1.83	2.73
1.68	2.67
1.92	2.72
1.68	2.55
1.74	2.75
1.69	2.75
1.62	2.71
1.77	2.74
1.64	2.58
1.68	2.87
1.58	2.93
1.60	2.87
1.70	2.75
1.73	2.59
1.75	2.92
1.72	2.82
1.60	2.88
1.74	2.78
1.62	2.77
1.78	
1.73	
1.71	

Table 3. Variation of the capacitance of a 10.5-inch-square paper analog with pressure

Pressure (inches of water)	Capacitance (farads x 10 ⁻⁸)
<1.0	0
1.2	3.66
2.1	4.21
4.2	4.71
6.0	5.02
8.1	5.30
9.2	5.51
10.3	5.62
12.2	5.77
13.2	5.88
133.	7.33

Table 4. End-to-end resistances of the boundary electrodes of some 10.5-inch-square paper analogs

Resistance (ohms)
5
3
3
10
5
7
6

Establishment of the validity of the analogs

Obviously, the reliable way to establish the validity of the paper analogs was to compare analog voltage transients with corresponding exact analytical solutions to Eq. 8 or Eq. 9. An exact solution in the form of a Fourier series was found in the literature (12, Eq. 22) for the problem consisting of two-dimensional flow within a square region having a uniform step input in potential applied along the entire perimeter. This problem assumes a uniform initial potential distribution within the section and no leakage to an environment. In a thermal system, this might be considered as the flow of heat within a bar of square cross section and having either infinite length or perfectly insulated ends. The bar, initially at uniform temperature, would have a step change in temperature applied to the entire lateral surface. It is convenient to consider the step input as an abrupt change from the initial potential (θ_0 or V_0) to zero, i.e., β changes from unity to zero. The square flow region (cross section of the bar) has sides of length $2s$, where s is the characteristic length. Thus, with the origin of the coordinate system at the center of the region, the absolute values of ξ and η vary between zero and unity. Expressed formally, the initial and boundary conditions of the problem are as follows:

$$\begin{aligned} \beta(\xi, \eta, 0) &= 1 & (-1 < \xi < 1, -1 < \eta < 1) \\ \beta(-1, \eta, \tau) &= 0, \quad \beta(1, \eta, \tau) = 0 & (-1 < \eta < 1, \tau > 0) \\ \beta(\xi, -1, \tau) &= 0, \quad \beta(\xi, 1, \tau) = 0 & (-1 < \xi < 1, \tau > 0). \end{aligned}$$

The flow region for this problem is represented by the large square of Fig. 7.

Numerical values of potential computed from the analytical solution to this problem are given in the above mentioned reference (12, Table 7) for the point which lies at the center of the region ($\xi = \eta = 0$). Numerical values of potential for other values of ξ and η involved in the present investigation were computed by the author from the same analytical solution.

It can be seen by symmetry from Fig. 7 that the investigation of only one octant is necessary to determine the potential distribution of the entire region. Also, it is apparent that the larger the length scale of the analog, the greater will be the accuracy in measuring distances on the analog. Because of these two considerations and one other to be discussed later, it was decided to utilize primarily analogs of only one quadrant of the region. For a given analog size, this would permit the use of a larger length scale than if the analogs were for the entire region. (There would be little, if any, gain in scale in simulating only one octant.) Thus the solid lines of Fig. 7 designate the region simulated by most of the analogs for this problem. The boundary electrode is indicated by the heavy band along the outside of the region.

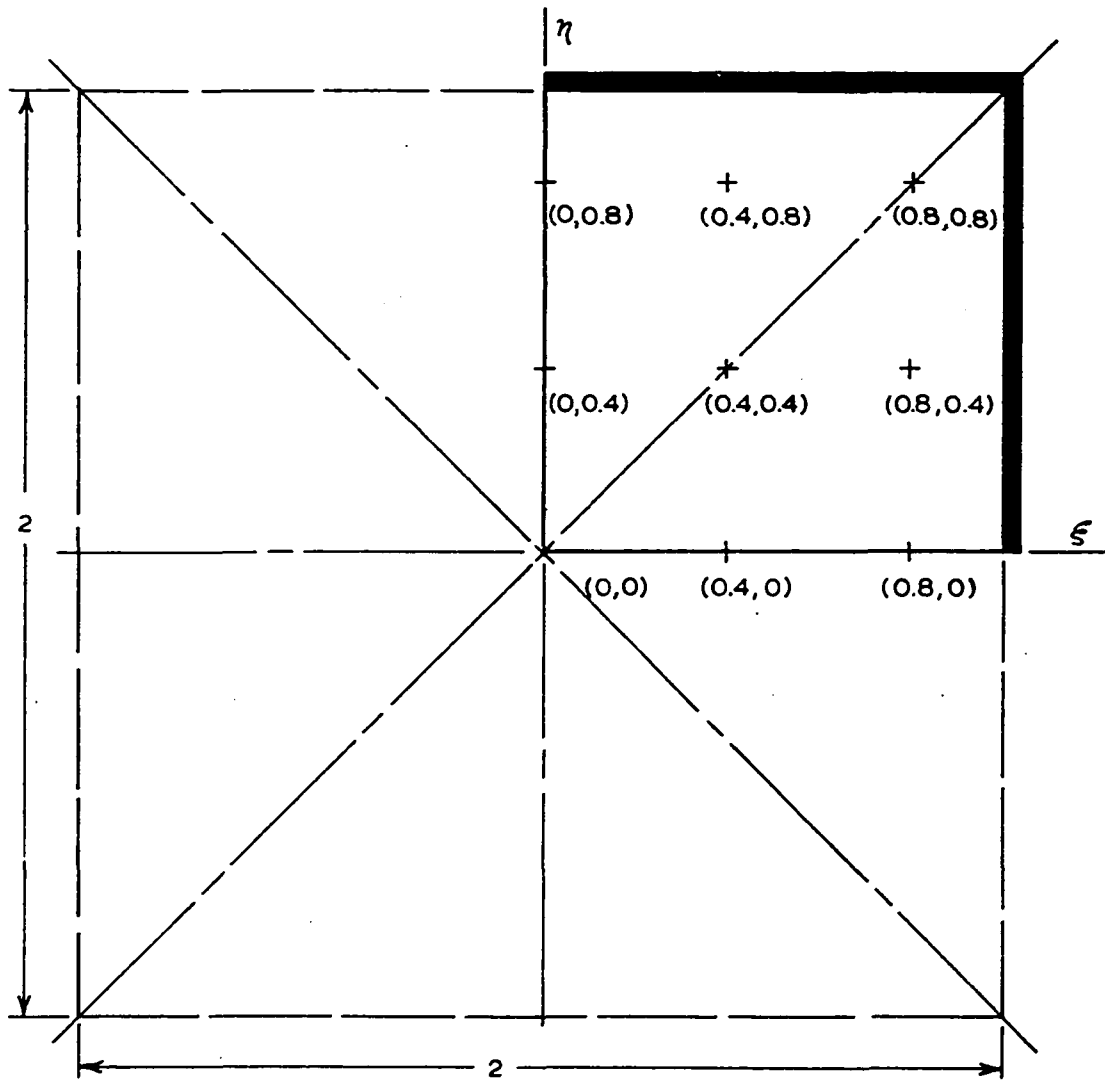


Fig. 7. Diagram of a square flow region

The nine points at which transients were usually obtained are indicated by crosses, the values of ξ and η for each such point being indicated nearby. By symmetry, the solutions at some points are identical to those at others, for example at (0.4, 0) and (0, 0.4). Specifically, the interchanging of coordinates gives a new point at which the solution is the same as at the original point.

The first set of analogs studied was used to establish the validity of the paper analogs. Each of these analogs had an effective flow region that was 10.00 inches square. In most cases, the boundary electrode along two adjacent sides was about 0.5 inch wide. The dimensionless time scale for each such analog was determined by matching (normalizing) the observed potential transient at (0, 0) to the numerical values of the exact analytical solution for this location. This same time scale was then used for the observed transients at other points on the given analog. Data from these transients appear in Table 5 and Fig. 8 along with the corresponding exact solution. The ranges of values of β at given values of ξ , η , and τ are indicated in Fig. 8 by the short vertical lines. In each case, the silver side of the paper faced upward except where the letter designating the analog is followed by (B), indicating that the black side faced upward.

To establish further the uniformity of response throughout an entire analog, transients were obtained from a 10.00-

Table 5. Distribution of potential, β , from the first set of paper analogs (time scales established by normalization to exact solution)

Location,		Time, τ	Exact solution	Potential, β								
ξ	η			Analogs:	A	B(B)	B	C	D	E	F	G
0	0	0.05	0.995		0.99	0.99	0.99	0.99	0.99	0.99	0.99	0.99
		0.10	0.901		0.90	0.90	0.90	0.90	0.90	0.90	0.90	0.90
		0.20	0.596		0.59	0.59	0.58	0.59	0.60	0.59	0.59	0.59
		0.30	0.368		0.37	0.37	0.37	0.37	0.37	0.37	0.37	0.37
		0.50	0.138		0.15	0.15	0.15	0.15	0.15	0.15	0.15	0.15
0.4	0.4	0.05	0.888		0.89	0.87	0.87	0.88	0.89	0.88	0.90	0.88
		0.10	0.670		0.66	0.65	0.65	0.66	0.67	0.66	0.67	0.66
		0.20	0.397		0.39	0.38	0.38	0.39	0.40	0.39	0.39	0.39
		0.30	0.242		0.24	0.24	0.25	0.24	0.24	0.24	0.24	0.24
		0.50	0.090		0.10	0.10	0.11	0.10	0.10	0.10	0.10	0.10
0.8	0.8	0.05	0.223		0.21	0.21	0.22	0.23	0.24	0.21	0.23	0.22
		0.10	0.119		0.12	0.12	0.12	0.13	0.13	0.11	0.12	0.12
		0.20	0.060		0.07	0.07	0.07	0.07	0.07	0.06	0.07	0.07
		0.30	0.035		0.04	0.05	0.04	0.05	0.05	0.03	0.04	0.04
		0.50	0.013		0.02	0.02	0.02	0.02	0.02	0.01	0.02	0.02
0.4	0	0.05	0.939		0.94	0.93	0.93	0.93	0.94	0.93	0.94	0.93
		0.10	0.777		0.77	0.76	0.76	0.77	0.77	0.77	0.77	0.77
		0.20	0.487		0.47	0.47	0.47	0.47	0.48	0.48	0.48	0.48
		0.30	0.301		0.30	0.30	0.30	0.30	0.30	0.30	0.30	0.30
		0.50	0.111		0.12	0.12	0.12	0.12	0.12	0.12	0.12	0.12
0	0.4	0.05	0.939		0.94	0.94	0.93	0.93	0.94	0.95	0.95	0.95
		0.10	0.777		0.78	0.77	0.77	0.77	0.77	0.78	0.78	0.78
		0.20	0.487		0.48	0.47	0.47	0.48	0.48	0.48	0.48	0.48
		0.30	0.301		0.30	0.30	0.30	0.30	0.30	0.30	0.30	0.30
		0.50	0.111		0.12	0.13	0.13	0.12	0.12	0.12	0.12	0.13

Table 5 (Continued).

Location,		Time, τ	Exact solution	Analog:			Potential, ϕ					
ξ	η			A	B(B)	B	C	D	E	F	G	
0.8	0	0.05	0.472	0.46	0.45	0.47	0.49	0.48	0.46	0.48	0.47	
		0.10	0.328	0.32	0.31	0.31	0.33	0.33	0.32	0.33	0.32	
		0.20	0.189	0.18	0.18	0.18	0.19	0.18	0.18	0.20	0.19	
		0.30	0.114	0.11	0.12	0.12	0.12	0.12	0.12	0.12	0.13	
		0.50	0.043	0.05	0.05	0.06	0.05	0.05	0.05	0.06	0.06	
0	0.8	0.05	0.472	0.47	0.47	0.47	0.46	0.46	0.48	0.48	0.49	
		0.10	0.328	0.32	0.32	0.32	0.32	0.31	0.32	0.33	0.33	
		0.20	0.189	0.19	0.19	0.18	0.19	0.18	0.18	0.19	0.19	
		0.30	0.114	0.12	0.12	0.12	0.12	0.12	0.12	0.12	0.12	
		0.50	0.043	0.05	0.06	0.06	0.05	0.05	0.05	0.05	0.06	
0.8	0.4	0.05	0.445	0.44	0.42	0.43	0.46	0.45	0.43	0.45	0.44	
		0.10	0.283	0.28	0.27	0.27	0.29	0.28	0.27	0.28	0.28	
		0.20	0.154	0.15	0.15	0.15	0.16	0.15	0.15	0.16	0.16	
		0.30	0.092	0.10	0.10	0.10	0.11	0.10	0.10	0.10	0.10	
		0.50	0.034	0.04	0.04	0.04	0.05	0.04	0.05	0.04	0.05	
0.4	0.8	0.05	0.445	0.42	0.43	0.43	0.43	0.43	0.43	0.45	0.44	
		0.10	0.283	0.27	0.27	0.27	0.27	0.27	0.27	0.28	0.28	
		0.20	0.154	0.15	0.16	0.15	0.16	0.15	0.15	0.16	0.16	
		0.30	0.092	0.09	0.10	0.10	0.10	0.09	0.09	0.10	0.10	
		0.50	0.034	0.04	0.04	0.04	0.05	0.04	0.04	0.05	0.05	

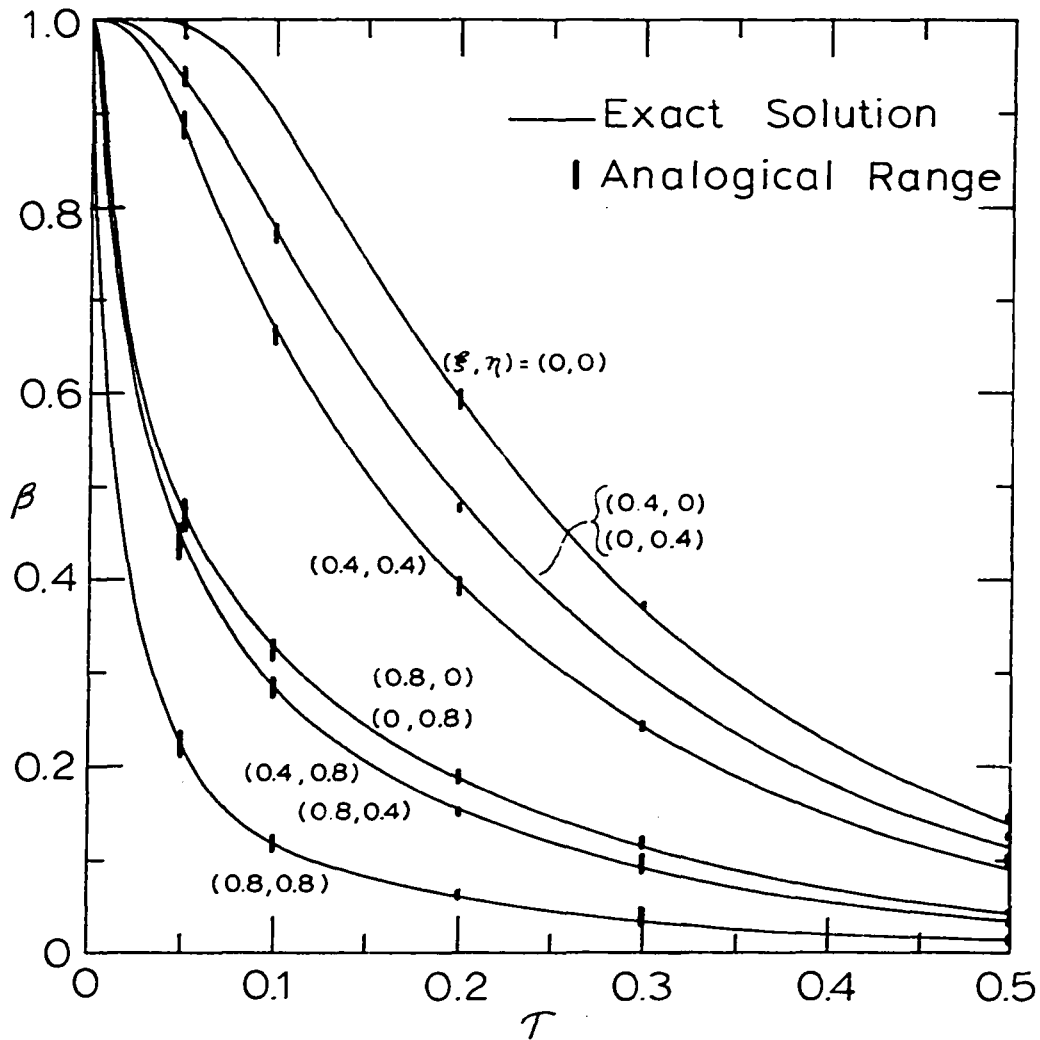


Fig. 8. Distribution of potential from the first set of paper analogs (analog time scales normalized)

inch-square analog which simulated the entire flow region of the problem described above, rather than just one quadrant. This involved the use of a boundary electrode around the entire perimeter of the resistance layer. The length scale, $x/\xi = s$, of this analog was only half as large as those of the first set of analogs. Thus the time scale, $t/\tau = Ks^2$, was only about one-fourth as large as the others, K being approximately the same for all the paper analogs at a given pressure. This time scale also was determined by the normalization process described above. To obtain oscilloscope traces similar in appearance to those from the first set, it was therefore necessary to use about a sweep rate about four times as great as before. Furthermore, the effective impedance of the analog as seen by the square-wave generator was much less than those of the first set. This resulted in a further deterioration of the generator output wave shape, for which adequate compensation could not be found. These two factors, higher sweep rate and increased generator output impedance, made it impossible to produce an input to the analog that even appeared to be a step. This circumstance constitutes the third consideration referred to previously which influenced the decision to utilize primarily analogs of only one quadrant of the flow region.

The results of the investigation upon the analog of the entire flow region are presented in Table 6 along with the

Table 6. Distribution of potential, ϕ , for an analog of an entire square flow region

Time, τ	Exact solution for step input	Potential, ϕ
		(Actual input)
0.05	0	0.14
0.10	0	0.08
0.20	0	0.04
0.30	0	0.03
0.50	0	0.01
		$\begin{pmatrix} \xi \\ \eta \end{pmatrix} = \begin{pmatrix} 0 \\ 0 \end{pmatrix}$
0.05	0.995	0.99
0.10	0.901	0.90
0.20	0.596	0.60
0.30	0.368	0.37
0.50	0.138	0.15
		$\begin{pmatrix} \xi \\ \eta \end{pmatrix} = \begin{pmatrix} 0.2 \\ 0.2 \end{pmatrix} \begin{pmatrix} 0.2 \\ -0.2 \end{pmatrix} \begin{pmatrix} -0.2 \\ 0.2 \end{pmatrix} \begin{pmatrix} -0.2 \\ -0.2 \end{pmatrix}$
0.05	0.976	0.97 0.97 0.97 0.97
0.10	0.845	0.86 0.85 0.84 0.84
0.20	0.542	0.55 0.54 0.53 0.53
0.30	0.333	0.34 0.34 0.33 0.33
0.50	0.124	0.14 0.14 0.13 0.13

Table 6 (Continued).

Time, τ	Exact solution for step input	Potential, ϕ							
$\begin{pmatrix} \xi \\ \eta \end{pmatrix} = \begin{pmatrix} 0.6 \\ 0.6 \end{pmatrix} \begin{pmatrix} 0.6 \\ -0.6 \end{pmatrix} \begin{pmatrix} -0.6 \\ 0.6 \end{pmatrix} \begin{pmatrix} -0.6 \\ -0.6 \end{pmatrix}$									
0.05	0.631	0.67	0.68	0.69	0.67				
0.10	0.395	0.44	0.44	0.45	0.43				
0.20	0.213	0.24	0.24	0.24	0.24				
0.30	0.128	0.15	0.15	0.15	0.15				
0.50	0.048	0.07	0.07	0.07	0.07				
$\begin{pmatrix} \xi \\ \eta \end{pmatrix} = \begin{pmatrix} 0.6 \\ 0.2 \end{pmatrix} \begin{pmatrix} 0.6 \\ -0.2 \end{pmatrix} \begin{pmatrix} 0.2 \\ 0.6 \end{pmatrix} \begin{pmatrix} 0.2 \\ -0.6 \end{pmatrix} \begin{pmatrix} -0.2 \\ 0.6 \end{pmatrix} \begin{pmatrix} -0.2 \\ -0.6 \end{pmatrix} \begin{pmatrix} -0.6 \\ 0.2 \end{pmatrix} \begin{pmatrix} -0.6 \\ -0.2 \end{pmatrix}$									
0.05	0.785	0.82	0.80	0.83	0.83	0.83	0.82	0.81	0.80
0.10	0.578	0.61	0.60	0.62	0.62	0.62	0.61	0.60	0.60
0.20	0.340	0.37	0.36	0.37	0.37	0.37	0.36	0.36	0.35
0.30	0.206	0.22	0.22	0.22	0.22	0.22	0.22	0.22	0.22
0.50	0.077	0.09	0.09	0.09	0.09	0.09	0.09	0.09	0.09

corresponding values from the exact solution for a step input and the values of input potential, showing the deviation from a step input. The effects of using a "rounded off" step input can be seen from the greater deviations from the exact solution than before.

As mentioned earlier, small spots of silver paint were coated on the top surface of the conductive paper at positions of contact with the probe electrodes. To demonstrate the need of these spots for proper contact, a comparison of results obtained from a given analog with and without the spots is made in Table 7. Corresponding values from the exact solution are also included.

Determination of time scales

As indicated previously, the values of dimensionless time, τ , for each analog in the first set were determined by normalizing the values of actual time, t , from the observed transient at one location to the exact solution for that location. In a practical application, this would of course not be possible since the exact solution to the problem being studied would usually not be known for any location. It is therefore necessary to devise some method of determining the time scale of a given analog independently of the solution to the problem being studied.

From Eq. 5, it is seen that the time scale, t/τ , depends

Table 7. A comparison of values of potential, β , obtained with and without contact paint spots

Location, ξ η		Time, τ	Exact solution	Potential, β without spots	With spots
0.4	0.2	0.05	0.931	0.97	0.92
		0.10	0.752	0.82	0.73
		0.20	0.464	0.51	0.44
		0.30	0.284	0.31	0.27
		0.50	0.106	0.13	0.11
0.6	0	0.05	0.792	0.86	0.79
		0.10	0.597	0.63	0.58
		0.20	0.357	0.37	0.34
		0.30	0.217	0.23	0.21
		0.50	0.081	0.11	0.09
0.8	0.6	0.05	0.376	0.52	0.36
		0.10	0.217	0.27	0.19
		0.20	0.113	0.12	0.10
		0.30	0.067	0.07	0.06
		0.50	0.025	0.03	0.03

upon the characteristic length, s , and the system field parameter (also called the time constant), $K = \bar{R}'\bar{C}'$. Accurate measurements of s , \bar{R}' , and \bar{C}' would thus permit a convenient determination of the time scale. Investigation was made into the possibility of determining the time scales of analogs in this manner. The time constant, K , for each of the analogs in the first set was computed from the directly measured values of \bar{R}' and \bar{C}' . The average value of $\bar{R}' = 1790$ ohms was used in each case. The constant, K , was also evaluated for each analog

in terms of corresponding actual and dimensionless times (see Eq. 5). This evaluation was facilitated by the normalization process made possible by a knowledge of the exact solution. The values of K thus determined are given in Table 8 along with the ratios of the values of K for each analog.

As can be seen from Table 8, for a given analog there is a definite discrepancy between the two values of K independently determined. Furthermore, the ratio between the values of K is clearly not a constant. Apparently, then, the measured values of \bar{R}' and \bar{C}' are not sufficiently accurate to use in the determination of the analog time scale.

A less direct procedure, involving "standard sheets" of conductive paper, was therefore adopted for determining time scales. With this procedure, a step control input of potential was applied at a given location on an analog of given size and shape. The resulting potential transient at another fixed location was observed. A given value of potential, β , should always occur at the same dimensionless time, τ , for every such analog regardless of its time constant. Thus, by once determining the values of τ corresponding to various values of β for the control transient, it should always be possible to determine the time scale, t/τ , and the time constant, K , of any such analog at a given pressure. Having determined the time scale of the analog, the sheet of conductive paper may be removed from the pressure apparatus and

Table 8. Time constant, K, for the first set of paper analogs

Analog	Time, $t \rightarrow \tau = 0.5$ (10^{-5} seconds)	\bar{C}' ($\frac{10^{-10}$ farads) (square inch)	Time constant, $K = \frac{t}{\tau a^2}$ $K = \bar{R}'\bar{C}'$ ($\frac{\text{microseconds}}{\text{square inch}}$)		Ratio = $\frac{t}{\tau a^2 \bar{R}'\bar{C}'}$
A	3.37	4.09	0.674	0.732	0.919
B(B)	4.01	4.67	0.802	0.836	0.960
B	3.46	4.04	0.692	0.723	0.958
C	3.51	4.42	0.702	0.791	0.888
D	3.40	4.38	0.680	0.784	0.868
E	3.42	4.46	0.684	0.798	0.857
F	3.56	4.41	0.712	0.789	0.904
G	3.56	4.53	0.712	0.811	0.878

trimmed to any desired size and shape. After the boundary electrodes are painted on, the sheet may be replaced into the pressure apparatus and the pressure restored to its original level.

It might be wondered whether the time scale (and hence time constant) of a given analog remains constant with pressure. Values of the time constant, K , as determined from the ratio t/τ are given in Table 9 for each of several analogs at times separated by intervals of the duration of hours, during which the paper was removed from the pressure apparatus. From this point on, the pressure was maintained at 12.0 inches of water, except when determining the effects of pressure changes.

The variations in the time constants of individual analogs indicated in Table 9 are not negligible. Values of K determined at smaller time intervals, again during which the paper was removed, are shown in Table 10. Here, the variations are much smaller than for the long time intervals. It was noted, however, that in some cases there was a noticeable rise in time constant during the first few minutes after a conductive sheet was replaced in the pressure apparatus. This effect can be seen from some of the values in Table 11.

Apparently some factor such as humidity is causing the long-term variation in K . Some sort of settling phenomenon is probably responsible for the variation shortly after paper replacement. It appears that there will be negligible varia-

Table 9. Time constants of some analogs determined at long time intervals

Analog	Time constant, $K = t/\tau$ (microseconds per square inch)		
A	0.645	0.649	0.598
B	0.629	0.641	0.629
C	0.689	0.709	0.699
D	0.658	0.694	0.685
E	0.654	0.694	0.694
F	0.685	0.719	0.725
G	0.685	0.714	0.694
	Time interval = 1 day		Time interval = 2-4 hours

Table 10. Time constants of some analogs determined at short time intervals (15-30 minutes)

Analog	Time constant, $K = t/\tau$ (microseconds per square inch)		
A	0.614	0.609	
G	0.714	0.714	0.725 0.725

Table 11. Variations in the time constants of some analogs shortly after paper replacement

Analog	Time constant, $K = t/\tau$ (microseconds per square inch)	
A	0.598	0.629
B	0.629	0.641
C	0.699	0.709
D	0.685	0.689
E	0.694	0.699
F	0.725	0.730
G	0.694	0.714
	Immediately after replacement	Less than ten minutes after replacement

tion due to removal and replacement if readings are taken between 15 and 30 minutes after replacement. This precaution was therefore taken from this point on.

As mentioned previously, the method chosen for the determination of analog time scales requires starting with sheets of paper of the same size and shape. It was decided to continue using 10.5-inch-square sheets. The location chosen for the control input was a corner of the sheet. The resulting control transient was observed at a point near the opposite

corner, 0.5 inch from the two adjacent sides. The values of τ corresponding to various values of β for the control transient were determined by using three such sheets (standard sheets) to match analogic solutions to the corresponding exact solution for a given problem. This problem consists of the two-dimensional flow within a circular region having a uniform step input applied along the entire circumference (uniform initial potential distribution and no leakage). (See Eq. 9.) In a thermal system, this might be considered as the flow of heat within a right circular cylinder with perfectly insulated ends, initially at uniform temperature, when a step change in temperature is applied on the entire lateral surface. Again for convenience, β is considered to change from unity to zero. Further, the radius of the circle is taken here as the characteristic lengths. Formally, the initial and boundary conditions may be expressed as follows:

$$\begin{aligned} \beta(\sigma, \alpha, 0) &= 1 & (0 < \sigma < 1, 0 \leq \alpha < 2\pi) \\ \beta(1, \alpha, \tau) &= 0 & (0 \leq \alpha < 2\pi, \tau > 0) \end{aligned}$$

Numerical values of the solution to this problem at the center of the region ($\sigma = 0$) were found in the literature (6, p. 266, Fig. 13-2 and Table 13-3). As with the square flow region, only one quadrant of the circular flow region was simulated.

For the calibration of the three standard sheets, the oscilloscope sweep rate first was adjusted so that the corre-

sponding values of horizontal position and β from the control transient were as indicated in Table 12. In each case, the oscilloscope time scale (time per unit horizontal displacement on the screen) was as shown in the second column of Table 13. After the control transient had been found for a given analog, the paper was removed and formed into a circular quadrant configuration. Upon replacement of the paper, the transient at the center of the circle was observed. Values for each such transient are given in Table 13.

These transients were fitted on the average as closely as possible to the corresponding theoretical solution as given by the solid line of the graph in Fig. 9. The ranges of β at

Table 12. The control transient

Horizontal position (oscilloscope screen) (inches)	Potential, β
0.10	0.90
0.20	0.72
0.40	0.47
0.60	0.32
1.00	0.15

Table 13. Calibration of the standard sheets

Sheet	Oscilloscope time scale (control) ($\frac{10^{-4} \text{ seconds}}{\text{inch}}$)	Observed transient at center (circular analog) Time, t (10^{-5} seconds)	Potential, β	Analog time scale, $\frac{t}{\tau}$ from fitting (10^{-5} seconds)	Time, τ from fitting	Time constant, K ($\frac{\text{microseconds}}{\text{square inch}}$)
H	3.10	0.62	0.91	7.94	0.078	0.794
		0.78	0.84		0.098	
		1.24	0.63		0.157	
		1.56	0.49		0.196	
		1.87	0.41		0.235	
		2.34	0.28		0.294	
		2.49	0.27		0.314	
		3.11	0.17		0.392	
		3.89	0.10		0.490	
J	2.94	0.59	0.92	7.55	0.078	0.755
		0.74	0.84		0.098	
		1.18	0.64		0.157	
		1.48	0.51		0.196	
		1.78	0.42		0.235	
		2.22	0.30		0.294	
		2.37	0.28		0.314	
		2.96	0.18		0.392	
		3.70	0.11		0.490	
K	3.11	0.62	0.92	7.96	0.078	0.796
		0.78	0.84		0.098	
		1.25	0.63		0.157	
		1.56	0.50		0.196	
		1.88	0.41		0.235	
		2.34	0.30		0.294	
		2.50	0.27		0.314	
		3.12	0.17		0.392	
		3.90	0.11		0.490	

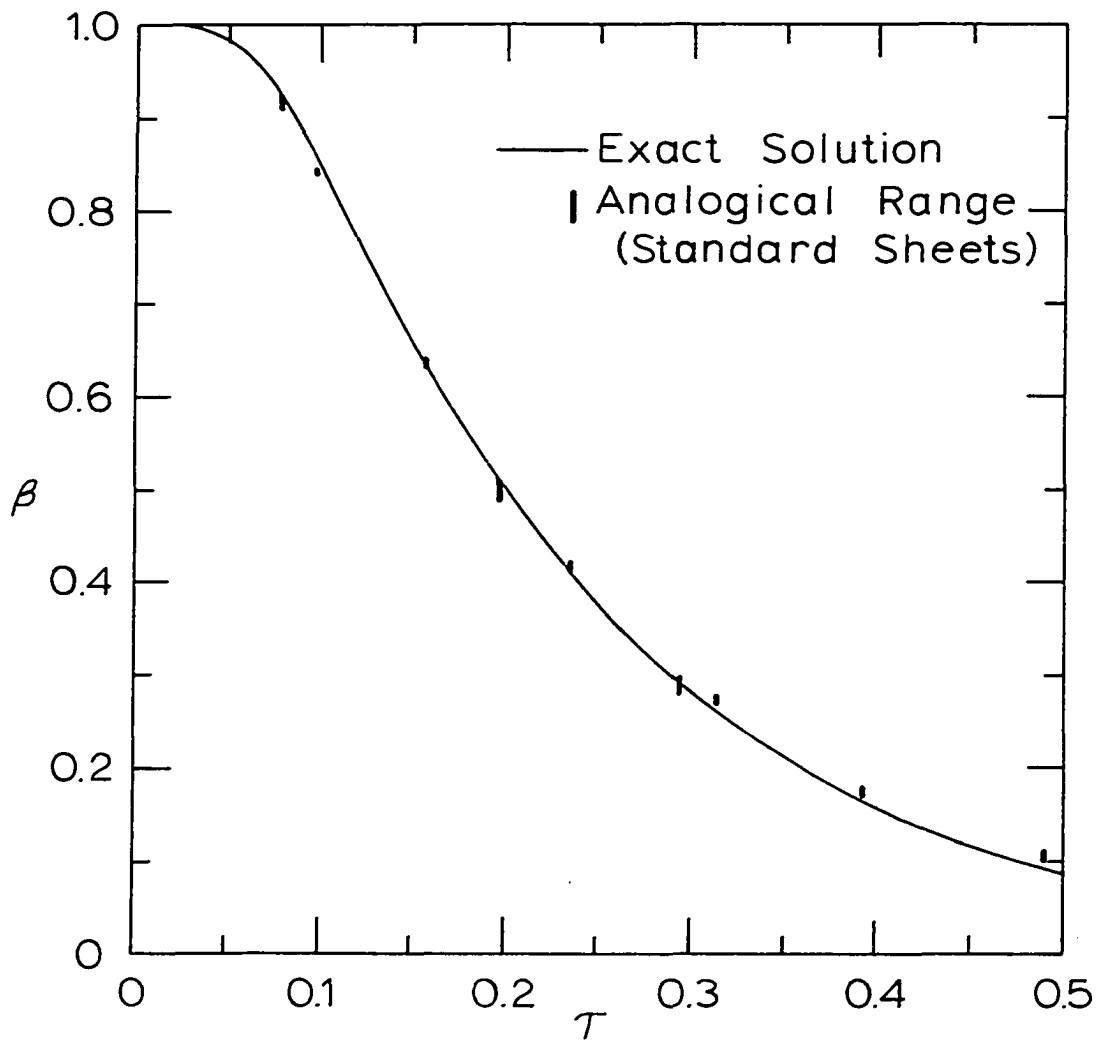


Fig.9. Potential transients at the center of a circular flow field

various values of τ from the fitted observed transients are indicated by the short vertical lines on the graph. The values of K resulting from this fitting process (see Eq. 5) are also listed in Table 13. From these values of K , it is possible to determine the values of τ corresponding to the various values of β for the control transient (see Eq. 5). For each of the three analogs, the value of τ corresponding to $\beta = 0.15$ was 3.90. Thus, for any sheet of the same dimensions as the standard sheets and with control transients applied and observed at the locations indicated, $\tau = 3.90$ should correspond to $\beta = 0.15$ for the control transient.

To check this procedure, several other sheets of conductive paper were cut to the dimensions of the standard sheets. The control transient was obtained from each sheet in the same manner as from the standard sheets and the value of K for the sheet at a given pressure obtained therefrom. These data are presented in Table 14.

Each sheet was subsequently used as the resistance layer for an analog of either a symmetrical square flow region or a quadrant of such a region. Transients were obtained at various points on each analog, the values of τ being determined from the value of K established as explained above. For each analog the oscilloscope time scale required for 1.00 inch to correspond to $\tau = 0.5$ (used for convenience) for the solution is also given in Table 14. Data from these transients

Table 14. Determination of the oscilloscope time scales for several square paper analogs

Sheet	Oscilloscope time scale (control)	Time constant, K	Width of analog	Characteristic length of analog	Oscilloscope time scale (solution) for 1.00 inch \rightarrow $\tau = 0.5$ ($\frac{10^{-5} \text{ second}}{\text{inch}}$)
	($\frac{10^{-4} \text{ seconds}}{\text{inch}}$)	($\frac{\text{microseconds}}{\text{square inch}}$)	(inches)	(inches)	($\frac{10^{-5} \text{ second}}{\text{inch}}$)
L	3.28	0.840	10.00	10.00	4.20
M	2.36	0.604	10.00	10.00	3.02
N	2.88	0.736	10.00	10.00	3.68
P	2.92	0.747	10.00	10.00	3.73
Q	2.69	0.689	10.00	5.00	0.862
R	0.971	0.690	6.00	6.00	1.24
S	1.88	0.753	8.00	8.00	2.41

appear in Tables 15 and 16 and Figure 10 along with the corresponding exact solution. The ranges of values of β at given values of ξ , η , and τ are indicated in Fig. 10 by the short vertical lines.

As a further indication of the effect of pressure upon the paper analogs, the variation of the time constant of a given analog with pressure is presented in Table 17 and Fig. 11.

Solution of a typical problem

The final investigation involving paper analogs consisted of determining the analogical solution of a "typical" problem for which no analytical solution was known by the author. This problem consisted of the two-dimensional flow within a circular region having a uniform step input applied along one half of the circumference (uniform initial potential distribution, no leakage). The initial and boundary conditions may be expressed formally as follows:

$$\begin{aligned} \beta(\sigma, \alpha, 0) &= 1 & (0 < \sigma < 1, 0 \leq \alpha < 2\pi) \\ \beta(1, \alpha, \tau) &= 0 & (\pi \leq \alpha \leq 2\pi, \tau > 0) \end{aligned}$$

A diagram of the configuration of the conductive-paper analog and the points at which transients were obtained are illustrated in Fig. 12.

Transients from three separate analogs of this problem

Table 15. Distribution of potential, β , from some 10.00-inch-square paper analogs (time scales determined independently of exact solution)

Location,		Time, τ	Exact solution	Potential, β			
ξ	η			Analog: L	M	N	P
0	0	0.05	0.995	0.98	0.98	0.98	0.98
		0.10	0.901	0.88	0.89	0.88	0.88
		0.20	0.596	0.58	0.59	0.57	0.57
		0.30	0.368	0.37	0.37	0.35	0.36
		0.50	0.138	0.15	0.16	0.14	0.14
0.4	0.4	0.05	0.888	0.87	0.87	0.87	0.87
		0.10	0.670	0.66	0.67	0.66	0.65
		0.20	0.397	0.39	0.40	0.40	0.39
		0.30	0.242	0.24	0.25	0.24	0.24
		0.50	0.090	0.10	0.11	0.10	0.10
0.8	0.8	0.05	0.223	0.24	0.21	0.23	0.21
		0.10	0.119	0.13	0.13	0.13	0.12
		0.20	0.060	0.07	0.07	0.08	0.07
		0.30	0.035	0.04	0.05	0.05	0.04
		0.50	0.013	0.02	0.02	0.02	0.02
0.4	0	0.05	0.939	0.91	0.93	0.93	0.92
		0.10	0.777	0.75	0.77	0.76	0.76
		0.20	0.487	0.47	0.50	0.47	0.47
		0.30	0.301	0.30	0.32	0.29	0.30
		0.50	0.111	0.12	0.13	0.11	0.12
0	0.4	0.05	0.939	0.93	0.93	0.92	0.93
		0.10	0.777	0.77	0.77	0.76	0.76
		0.20	0.487	0.48	0.49	0.47	0.47
		0.30	0.301	0.30	0.31	0.30	0.30
		0.50	0.111	0.12	0.13	0.12	0.12

Table 15 (Continued).

Location,		Time, τ	Exact solution	Analog: L	Potential, ϕ		
ξ	η				M	N	P
0.8	0	0.05	0.472	0.45	0.46	0.46	0.46
		0.10	0.328	0.31	0.33	0.32	0.32
		0.20	0.189	0.19	0.20	0.19	0.19
		0.30	0.114	0.12	0.11	0.12	0.12
		0.50	0.043	0.05	0.07	0.05	0.06
0	0.8	0.05	0.472	0.47	0.45	0.46	0.46
		0.10	0.328	0.33	0.32	0.32	0.32
		0.20	0.189	0.20	0.19	0.20	0.19
		0.30	0.114	0.12	0.12	0.12	0.12
		0.50	0.043	0.05	0.06	0.06	0.06
0.8	0.4	0.05	0.445	0.42	0.42	0.45	0.42
		0.10	0.283	0.27	0.28	0.29	0.28
		0.20	0.154	0.16	0.17	0.17	0.16
		0.30	0.092	0.10	0.11	0.10	0.10
		0.50	0.034	0.04	0.05	0.05	0.04
0.4	0.8	0.05	0.445	0.45	0.44	0.45	0.43
		0.10	0.283	0.29	0.29	0.30	0.28
		0.20	0.154	0.17	0.17	0.17	0.16
		0.30	0.092	0.10	0.11	0.11	0.10
		0.50	0.034	0.04	0.05	0.05	0.04

Table 16. Values of potential, β , for some paper analogs of smaller characteristic length (time scales determined independently of exact solution)

Location, ξ η		Time, τ	Exact solution	Analogs: Q	Potential, β		
					R	S	
0	0	0.05	0.995	0.98	0.99	0.98	
		0.10	0.901	0.90	0.90	0.90	
		0.20	0.596	0.61	0.61	0.60	
		0.30	0.368	0.39	0.40	0.39	
		0.50	0.138	0.16	0.17	0.17	

Table 17. Variation of the time constant of a paper analog with pressure

Pressure (inches of water)	Time constant, K ($\frac{\text{microseconds}}{\text{square inch}}$)
<1.0	0
1.0	0.449
2.0	0.485
4.0	0.555
8.0	0.606
12.0	0.641
16.0	0.667
133.	1.09

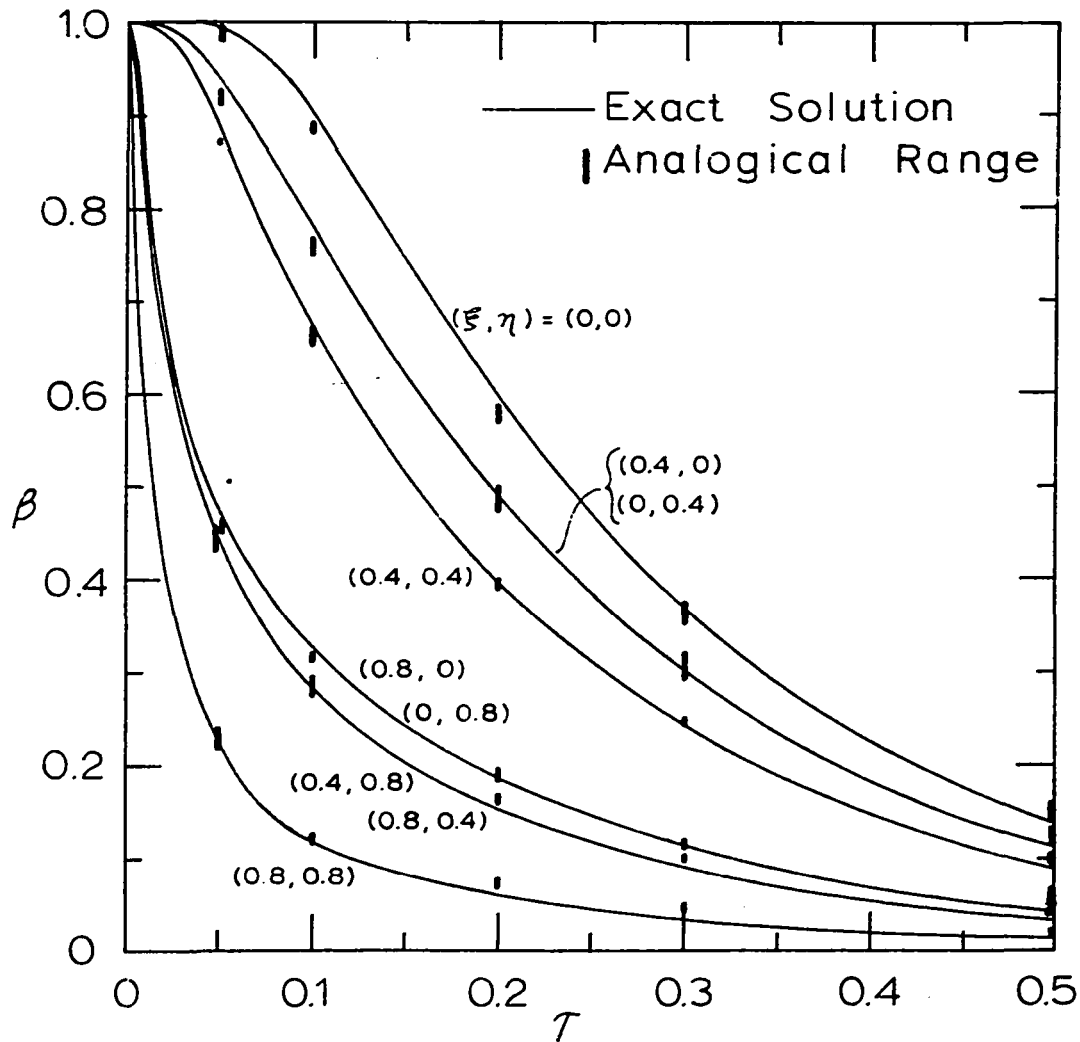


Fig. 10. Distribution of potential from some 10.00-inch-square paper analogs (analog time scales not normalized)

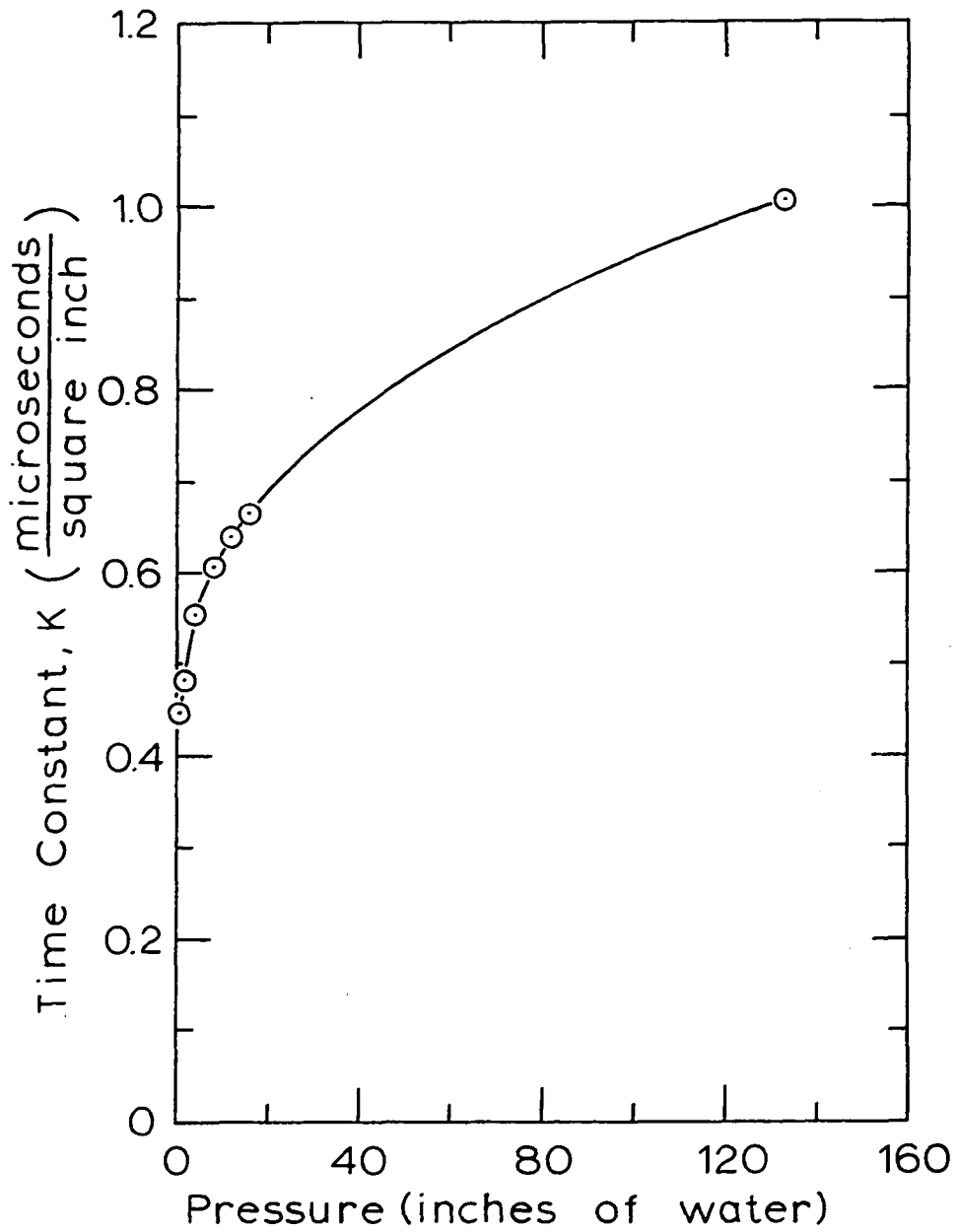


Fig. 11. Variation of the time constant of a paper analog with pressure

⊕ Points at which transients were obtained

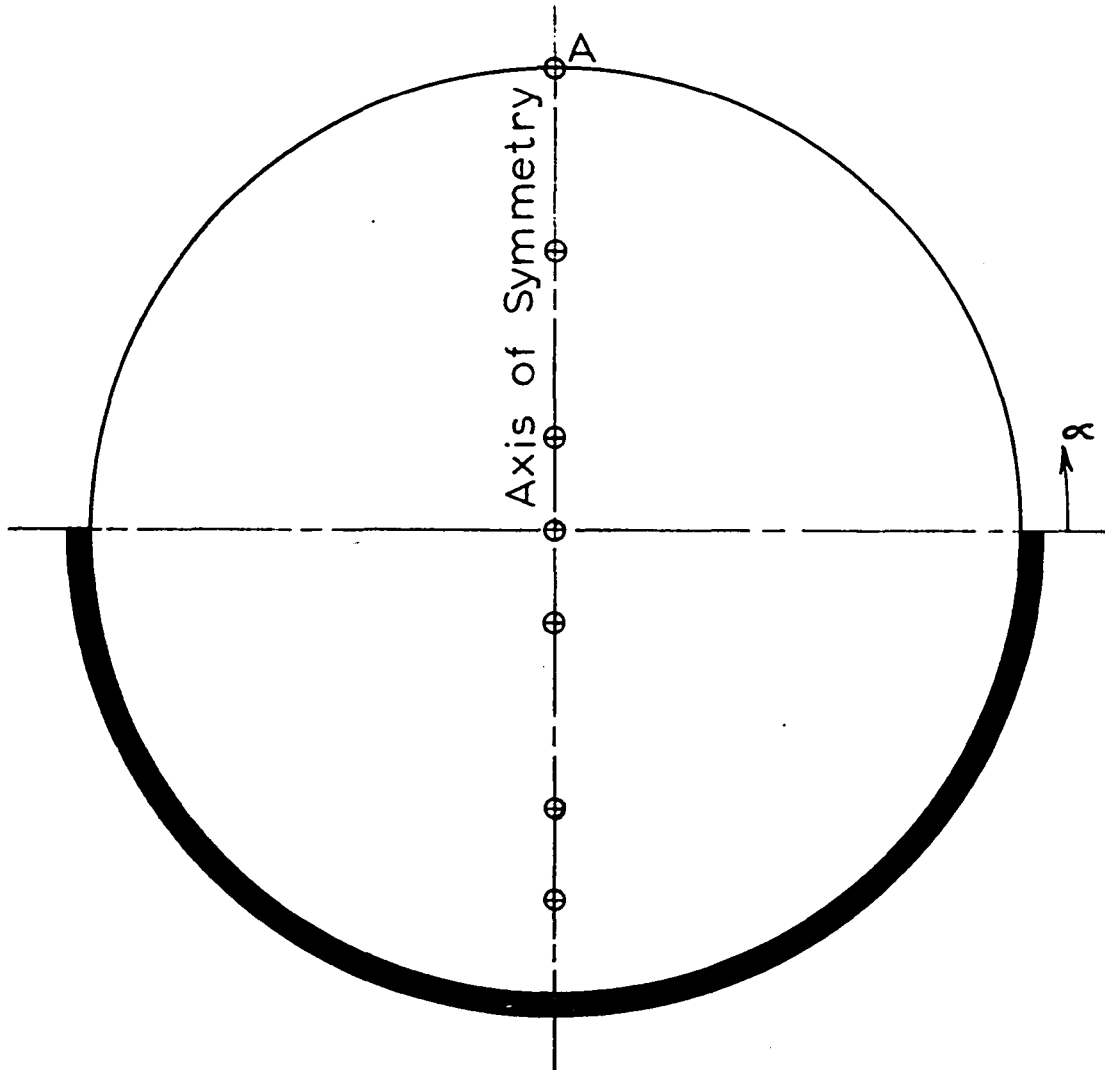


Fig. 12. Configuration of the analog for a typical problem

were obtained. For each analog, data pertaining to the determination of the oscilloscope time scale required for 1.0 inch on the screen to correspond to $\tau = 0.5$ for the solution are given in Table 18. Observed values of potential from points along the axis of symmetry of each of the three analogs are presented in Table 19. Some of these values are plotted against time in Fig. 13 to indicate representative transients along the axis of symmetry. Some of the values of Table 19 are plotted against distance in Fig. 14 to show the distribution of potential along the axis of symmetry at given instants of time.

Mention should be made of some of the likely sources of error in the investigation of paper analogs in addition to the nonuniformities already discussed. The oscilloscope traces were always read at a vertical grid line, thus minimizing errors in time readings. However, it is estimated that the observation of the vertical position of a trace could be in error by as much as $\Delta\beta = 0.01$ or 0.02 . Further error may have been introduced by the difficulty in adjusting the bounds of the trace to given grid lines. Errors in oscilloscope calibration or linearity might have caused additional error.

Conductive-Paint Analog

To determine the uniformity of the resistance layers of paint analogs, a measurement was made of the resistances of

Table 18. Determination of the oscilloscope time scales for analogs of a typical problem (diameter = characteristic length = 10.00 inches)

Sheet	Oscilloscope time scale (control)	Time constant, K	Oscilloscope time scale (solution) for 1.00 inch \rightarrow $\tau = 0.5$ ($\frac{10^{-5}$ seconds) inch
	($\frac{10^{-4}$ seconds) inch	($\frac{\text{microseconds}}$ square inch)	
T	2.84	0.728	3.64
U	2.67	0.683	3.41
V	2.72	0.695	3.47

several short rectangular strips, one inch wide, of coats of conductive paint. The results of these measurements are presented in Table 20. The average of the values of \bar{R}' for R11 paint was 4400 ohms, the average deviation from the mean being 500 ohms. By way of comparison, the resistance per square of a coat of the higher resistance R21 paint was of the order of 230,000 ohms.

One of the factors affecting the uniformity of resistance is the smoothness with which the paint may be applied. It was found that fresh R11 paint streaked quite badly when applied, making it almost impossible to produce a layer that even looked uniform. In addition, it rubbed and flaked off the sheet plastic very readily after drying. It was noted that

Table 19. Distribution of potential, β , from analogs of a typical problem along the axis of symmetry

Location, σ	Time, τ	Analog: T	Potential, β		Average
			U	V	
-0.8	0.05	0.15	0.16	0.16	0.16
	0.10	0.09	0.09	0.09	0.09
	0.20	0.05	0.05	0.05	0.05
	0.30	0.03	0.03	0.03	0.03
	0.50	0.01	0.01	0.01	0.01
-0.6	0.05	0.29	0.30	0.30	0.30
	0.10	0.17	0.17	0.18	0.17
	0.20	0.10	0.09	0.09	0.09
	0.30	0.05	0.06	0.05	0.05
	0.50	0.02	0.02	0.02	0.02
-0.2	0.05	0.58	0.59	0.60	0.59
	0.10	0.37	0.37	0.37	0.37
	0.20	0.20	0.20	0.19	0.20
	0.30	0.11	0.11	0.11	0.11
	0.50	0.05	0.05	0.04	0.05
0.2	0.05	0.80	0.80	0.81	0.80
	0.10	0.57	0.57	0.57	0.57
	0.20	0.31	0.30	0.29	0.30
	0.30	0.18	0.17	0.16	0.17
	0.50	0.07	0.07	0.06	0.07
0.6	0.05	0.92	0.91	0.91	0.91
	0.10	0.71	0.70	0.68	0.70
	0.20	0.40	0.37	0.36	0.38
	0.30	0.23	0.21	0.19	0.21
	0.50	0.08	0.08	0.07	0.08
1.0	0.05	0.95	0.94	0.96	0.95
	0.10	0.76	0.74	0.76	0.75
	0.20	0.43	0.40	0.40	0.41
	0.30	0.24	0.23	0.22	0.23
	0.50	0.09	0.08	0.08	0.08

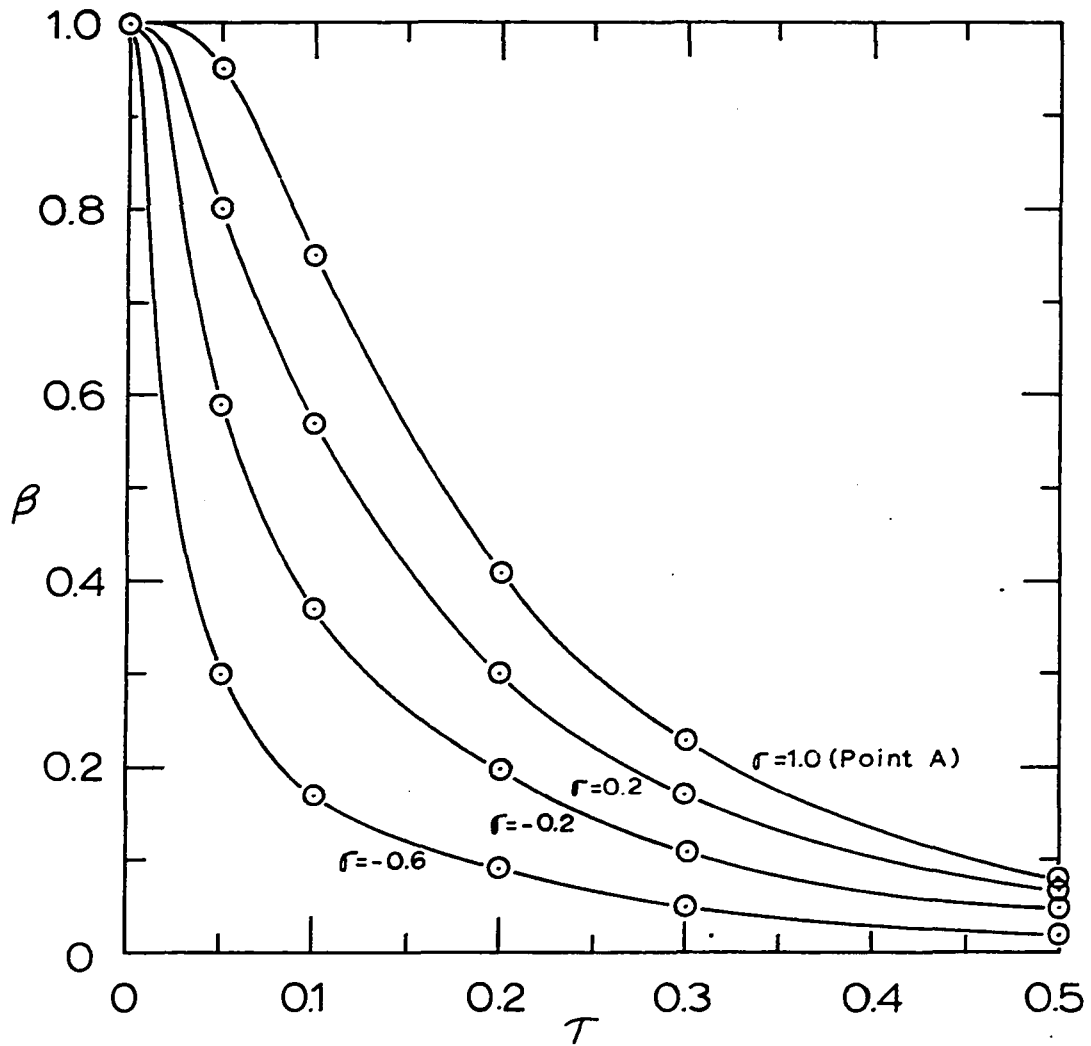


Fig. 13. Representative analog transients for a typical problem (axis of symmetry: $\alpha = \frac{\pi}{2}$)

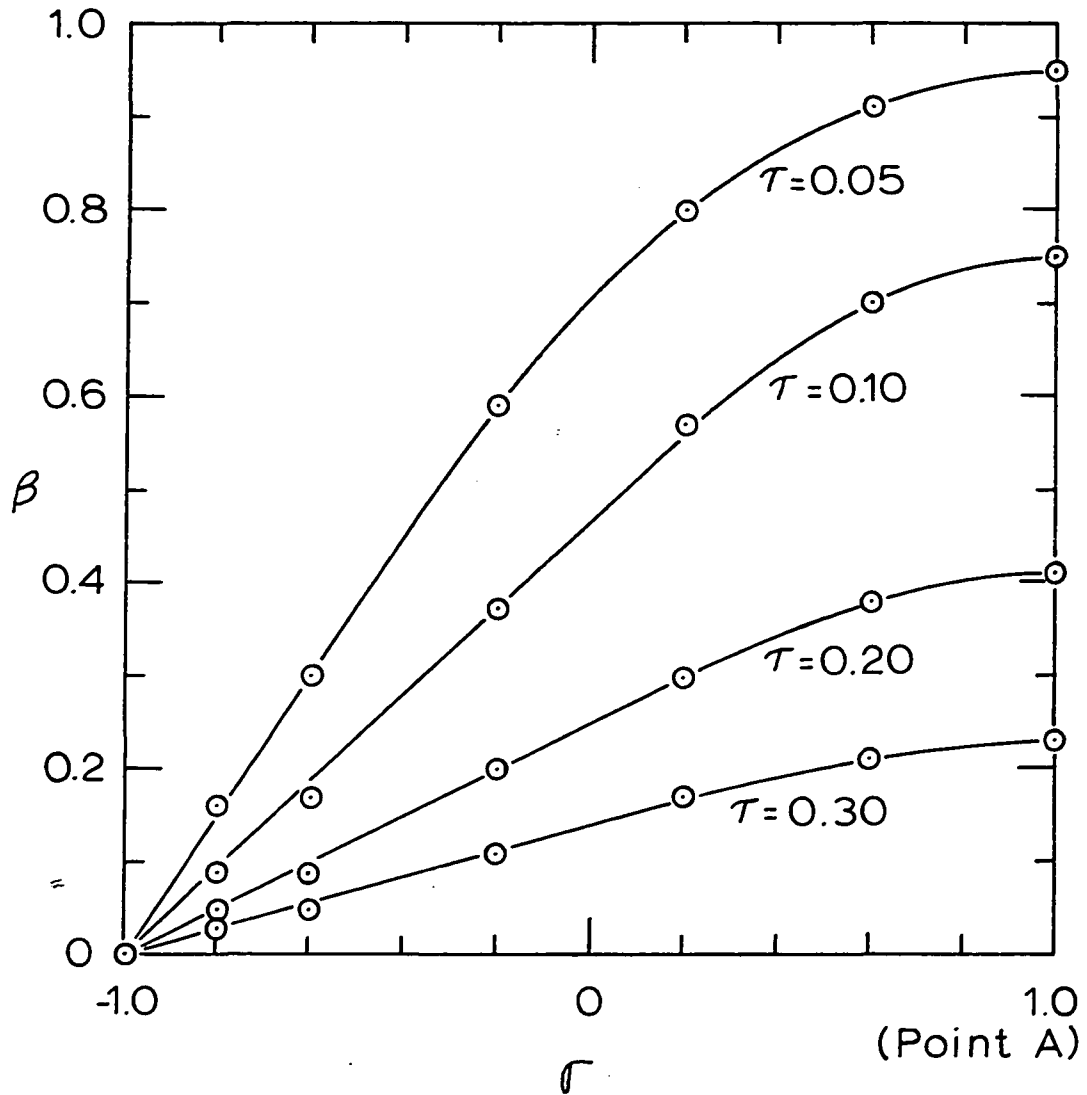


Fig. 14. Distribution of analog potential along the axis of symmetry ($\alpha = \frac{\pi}{2}$) of a typical problem

Table 20. Resistances of one-inch strips of conductive paint

	Strip length (inches)	Total resistance (ohms x 10 ³)	Resistance per square (ohms x 10 ³)
R21 Paint	8.8	2000.	230.
R11 Paint	1.54	7.5	4.9
"	1.38	6.1	4.4
"	1.38	6.2	4.5
"	1.41	5.4	3.8
"	1.39	5.3	3.8
"	1.41	5.5	3.9
"	1.38	6.8	4.9
"	1.75	6.8	3.9
"	2.02	7.8	3.9
"	1.53	7.5	4.9
"	1.34	7.0	5.2
"	1.42	6.5	4.6
"	1.41	6.6	4.7
"	1.38	4.9	3.6
"	1.42	5.4	3.8
"	1.41	6.5	4.6
"	1.71	8.9	5.2
"	1.94	9.8	5.0

the streaking seemed to be related to the extremely fast drying of the paint. By trial and error, it was subsequently found that this undesirable behavior of the paint could be minimized by the following process.

First the paint was dried by allowing much of the existing solvent to evaporate. The paint was then thinned out again by the addition of SL-2 Very-Slow-Drying Solvent (Micro-Circuits Company). The resulting mixture flowed like enamel, brush marks being hardly noticeable. The resulting layer was also much more durable when dried.

To determine the uniformity of the dielectric layers, measurements were made of the capacitances of several rectangular capacitors. The results of the measurements are presented in Table 21. Most of these capacitors were formed, as indicated previously, by coating both surfaces of a plastic sheet with regions of silver paint. The average value of \bar{C}' for these capacitors was 2170 micromicrofarads per square inch, the average deviation from the mean being 30 micromicrofarads per square inch. The value of \bar{C}' for a capacitor formed by placing one of the coats of silver paint over a resistance layer was found to be 2420 micromicrofarads per square inch.

In measuring the resistance between a boundary electrode and the ground layer of a conductive-paint analog (to check assumption (b)), it was observed that the ohmmeter needle

Table 21. Capacitances of rectangular sections of conductive-paint analogs

	Length	Width	Total capacitance	Capacitance per unit area, \bar{C} '
	(inches)	(inches)	(farads x 10^{-9})	($\frac{\text{farads x } 10^{-9}}{\text{square inches}}$)
With Resistance Layer	14.8	1.00	35.8	2.42
Without Resistance layer	3.52	2.80	21.3	2.16
"	1.65	1.13	4.12	2.22
"	1.55	1.13	3.70	2.12
"	1.64	1.22	4.33	2.16
"	1.57	1.20	4.11	2.18

deflected momentarily, apparently during the build-up of charge on the resistance and ground layers. In some cases, no steady-state deviation of the meter needle from the infinity reading on the highest scale (X10,000) could be detected. In other cases (discarded as analogs), there was a finite resistance of the same order of magnitude as along the resistance layer. The corresponding conductance was obviously not negligible in these cases. It should be noted that in some of these latter cases, pinholes were noticed in the plastic sheet following the application of paint on one surface. Very likely, the leakage here resulted from short circuits between the resistance and ground layers. Furthermore, it was observed that the paint thinner chemically attacked the plastic. Specifically, rubbing the plastic with a cloth impregnated with thinner caused the plastic to appear cloudy rather than transparent. The subsequent coating of both surfaces of one such region of plastic sheet with conductive paint resulted in a finite resistance through the region.

To check assumption (e), the resistance was measured from end to end of the boundary electrode (about an eighth of an inch wide) which extended along half the circumference of a circular resistance layer. This resistance was approximately 100 ohms as compared with an \bar{R}' of about 4000 ohms for the resistance layer.

As with the paper analogs, potential transients from the

paint analogs were compared to corresponding exact analytical solutions. Numerical values for an exact solution in the form of a Fourier series were found in the literature (1, p. 101, Fig. 11) for the problem consisting of one-dimensional flow with the same step input at both ends of the flow region-- uniform initial potential distribution and no leakage. (See Eq. 7.) It is convenient to consider the step input as an abrupt change from the initial potential (θ_0 or V_0) to zero, i.e., β changes from unity to zero. (The initial potential is used as the characteristic potential.) The length of the flow region extends a distance s on either side of the origin of the coordinate system, where s is the characteristic length. Hence the absolute value of β varies between zero and unity. Expressed formally, the initial and boundary conditions are as follows:

$$\beta(\xi, 0) = 1 \quad (-1 < \xi < 1)$$

$$\beta(-1, \tau) = 0 \quad (\tau > 0)$$

$$\beta(1, \tau) = 0 \quad (\tau > 0)$$

Values of β at various times and positions obtained from transients in several one-dimensional conductive-paint strip analogs are presented in Table 22. These data are summarized in Fig. 15, their ranges being indicated by the heavy vertical lines. The corresponding exact solution is represented by the solid lines of Fig. 15.

Another problem for which analog potential transients

Table 22. Distribution of potential, ϕ , in one-dimensional conductive-paint strip analogs

Location, ξ	Time, τ	Exact solution	Analog:					
			A	B	Potential, ϕ		E	F
			C	D				
0	0.10	0.948	0.910	0.905	0.910	0.910	0.965	
	0.20	0.773	0.735	0.710	0.720	0.720	0.770	0.755
	0.40	0.476	0.470	0.460	0.465	0.465	0.470	0.455
	0.60	0.287	0.310	0.300	0.290	0.290		0.280
	1.00	0.110	0.140	0.130	0.125	0.115	0.110	0.110
0.60	0.10	0.630	0.640	0.655	0.650			
	0.20	0.466	0.470	0.475	0.480			
	0.40	0.276	0.290	0.290	0.300			
	0.60	0.171	0.185	0.190	0.185			
	1.00	0.067	0.085	0.070	0.070			
0.85	0.10	0.260	0.265	0.300	0.350			
	0.20	0.186	0.185	0.190	0.215			
	0.40	0.110	0.120	0.100	0.125			
	0.60	0.066	0.075	0.060	0.065			
	1.00	0.027	0.035	0.010	0.015			

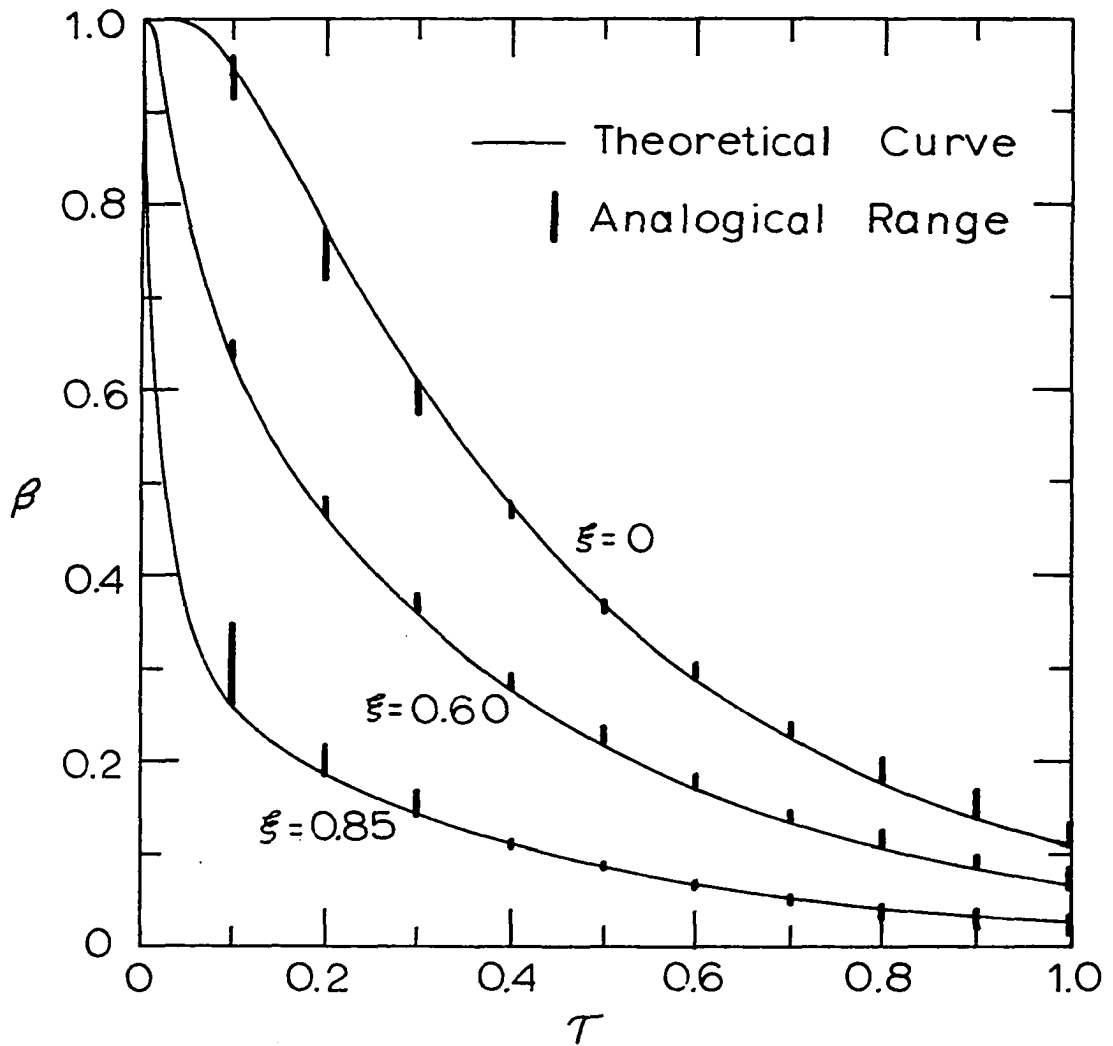


Fig.15. Potential transients for a one-dimensional flow field

were compared to the corresponding exact solution is that of the two-dimensional flow within a circular region having a uniform step input applied along the entire circumference. This problem was described in detail earlier. In Fig. 16, a semi-logarithmic plot is presented of the variation of β with τ at the center of the circle. As before, the exact solution is represented by a solid line and corresponding data from a paint analog are shown as isolated points.

It should be noted that the values of dimensionless time for the analog data shown in Figs. 15 and 16 were determined for each analog by a matching of the oscilloscope trace obtained at $\xi = 0$ or $\sigma = 0$ with the corresponding values from the analytical solution.

Electrolytic Analog

A third problem for which an exact solution was found (2, p. 110, 111) is one which is identical to the one dimensional problem described earlier in this section (Fig. 15) except for the presence of leakage to an environment of $\beta_e = 0$. In terms of the dimensionless variables defined earlier, this solution is

$$\beta(\xi, \tau) = e^{-H\tau} \beta_1(\xi, \tau) \quad (11)$$

where β_1 is the solution to the one-dimensional problem without leakage (see Eq. 7 and Fig. 15).

An attempt was made to simulate this problem by means of

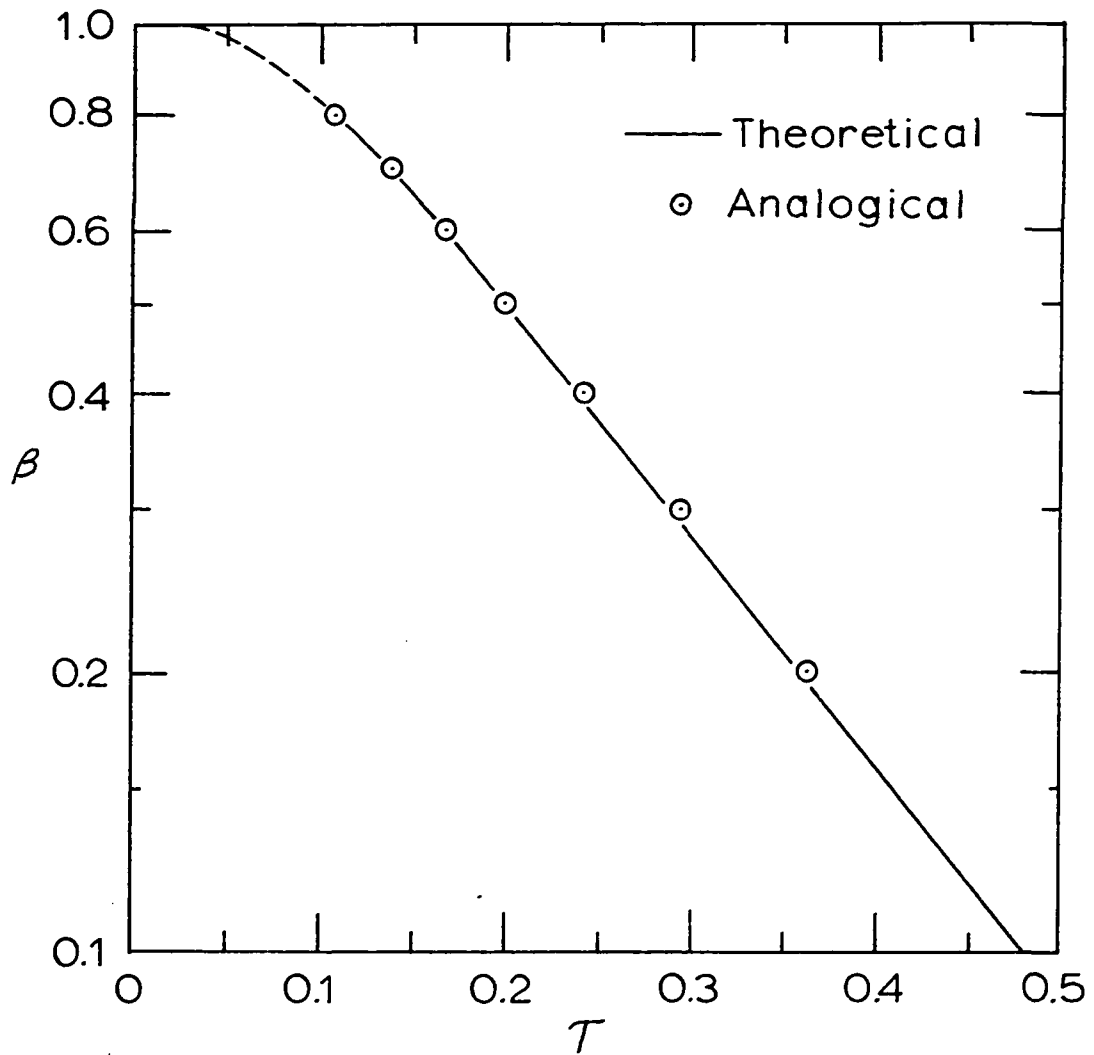


Fig.16. Potential transient at the center of a circular flow field

an electrolytic strip analog. It was not found possible to simulate exactly the initial condition of this problem. The initial distribution of potential along the strip, instead of being uniform, was

$$\beta(\xi, 0) = \beta_0 \cosh \sqrt{H} \xi \quad (12)$$

where

$$\beta_0 = \frac{1}{\cosh \sqrt{H}} \quad (13)$$

was the value of the potential at the center ($\xi = 0$). Equation 12 is the steady-state solution of the one-dimensional flow problem with leakage when $\beta_e = 0$ and $\beta(-1) = \beta(1) = 1$. The value of H can be determined from Eq. 13 if β_0 is known.

Photographs of oscilloscope traces of transients at three locations on the analog used are given in Fig. 17. These traces were so positioned relative to the grid that $\beta = 1$ is two large divisions above the horizontal axis and $\beta = 0$ is two divisions below the axis. The initial value of the transient at $\xi = 0$ gives $\beta_0 = 0.90$, the corresponding value of H being 0.22.

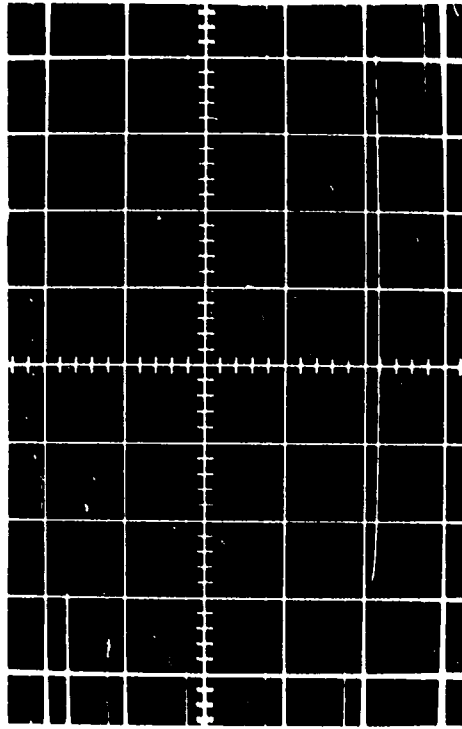
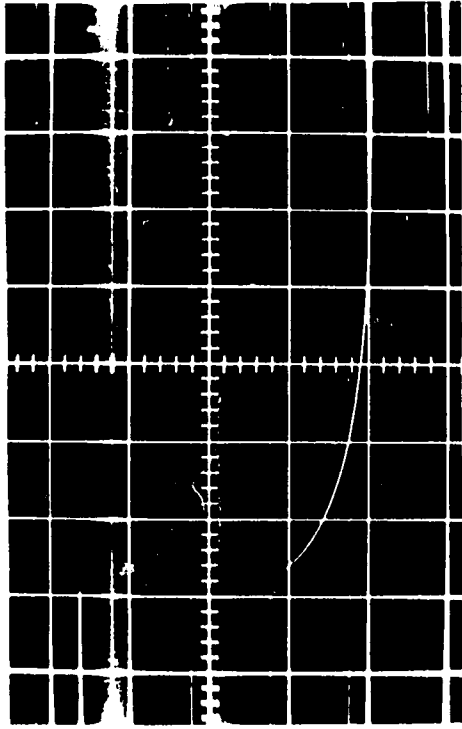
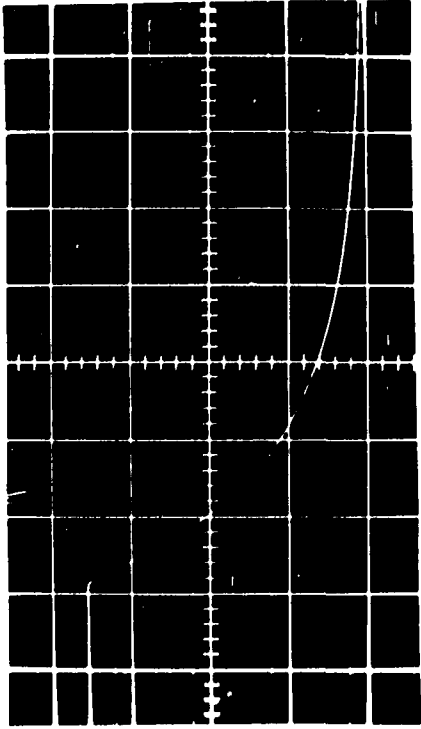
The time scale of the photographs was interpreted to be such that one large division corresponded to $\Delta\tau = 0.27$. Values from the photographic curves for $\xi = 0$ and $\xi = 0.81$ and the corresponding theoretical transients are plotted in Fig. 18.

a. $\xi = 0$

b. $\xi = 0.81$

c. $\xi = 1 - \epsilon$ (immediately
adjacent to the electrode)

Fig. 17. Photographs of oscilloscope traces of transients from a one-dimensional electrolytic strip analog



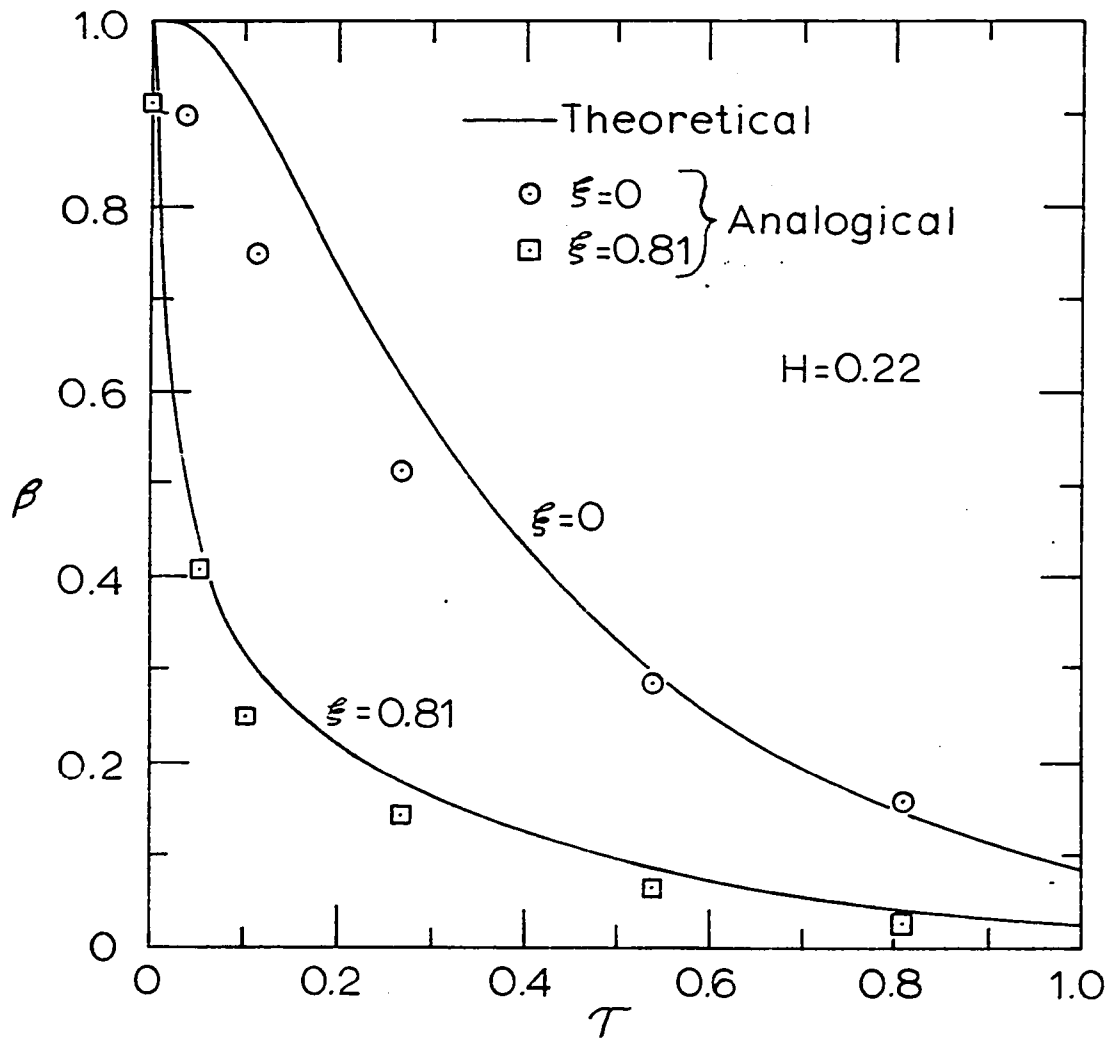


Fig.18. Potential transients for a one-dimensional flow field with leakage

It should be noted that although the step input was from $\beta = 1$ to $\beta = 0$, the potential of the analog drops below $\beta = 0$, especially at points close to the electrodes, as illustrated in Fig. 17 by the photograph for $\xi = 1 - \epsilon$. Apparently this phenomenon is the result of a contact potential between the electrodes and the electrolyte and at the present time is one of the major drawbacks to the electrolytic type of analog.

In obtaining the various transients, it was observed that the measurement of the location of the probe in regions near electrodes is critical. This results from the fact that the potential gradient is relatively high in such regions.

Suggestions for Future Study

It is recommended that future investigations with paper analogs be conducted with the higher resistance "Teledeltos" paper which is available. This would increase the time constant by about a factor of ten and thus reduce the required oscilloscope sweep rate by the same factor. In addition, the loading of the generator by the analog would be considerably minimized.

Further study should be given to the possible use of much higher pressures than were involved in the present investigation. It is felt that the uniformity of capacitance might be thereby increased.

The development of an effective technique for uniformly

spraying conductive paint might well be investigated. It is felt that the major difficulty encountered in spraying with commercial sprayers is the unsteadiness of flow through the nozzle. Custom-made nozzles might sufficiently minimize this problem.

Considerable development of the electrolytic analogs remains to be done before they will prove satisfactory. One of the major drawbacks of these analogs is the rapid drying of the electrolyte. It would probably be worthwhile to give detailed study to the following factors: (a) proportions of constituents of the electrolyte, including water; (b) thickness of the layer of electrolyte; (c) pouring temperature of the electrolyte; (d) time interval between pouring and taking data; (e) uniformity of the electrolyte; (f) contact between electrolyte and electrodes.

The usefulness of the continuous-medium analogs might be greatly increased by extending their application to problems involving field coefficients which are functions of position. A study of this possibility as well as the effects of sources and sinks would seem desirable.

SUMMARY AND CONCLUSIONS

Unsteady flow fields may exist in various kinds of physical systems such as thermal, hydrodynamical, and electrical. The equations governing such systems are identical in form and therefore formal analogies exist among the systems. Because of the convenience of making measurements upon electrical systems, it is desirable to use electrical devices as analogs or models of the other types of systems.

A basic design for an electrical analog to simulate two-dimensional unsteady-flow fields has been conceived which would be geometrically similar to the system of interest. This design involves three distinct layers: a resistance layer; a dielectric layer; and a ground layer. Such geometrical analogs could be more advantageous to use than the widely used equivalent finite-difference networks because of the combination of good accuracy and simplicity (hence economy) potentially inherent within them.

Three types of analogs of the above-mentioned basic design have been studied. The type studied most extensively utilizes conductive paper, sheet plastic, and conductive paint. A second type utilizes conductive paint, applied by brush, and sheet plastic. These two types are applicable to fields without leakage. A third type of analog studied, applicable to fields involving leakage to or from a surface environment,

utilizes an electrolyte and anodized aluminum foil. Voltage transients from analogs of certain simple problems were obtained and compared with corresponding exact analytical solutions.

The maximum deviation of data from 10.0-inch-square conductive paper analogs from the exact solution was about 55% of the exact value. However, this deviation amounted to less than 2% of the applied step input. Deviations as high as 2.9% of the applied step input were observed.

To illustrate the usefulness of the geometrical analogs, a somewhat more complex flow problem was simulated by a conductive-paper analog, and data obtained therefrom were presented. This problem consisted of flow within a circle, along one half of whose circumference a step input was applied.

Potential transients from a few conductive-paint analogs were compared with the corresponding exact solutions. Deviations as high as 60% of the exact values and as high as 9% of the applied input were observed. These were probably due to the considerable lack of uniformity of the conductive-paint resistance layer. Efforts to improve the uniformity by spraying the paint were unsuccessful.

Potential transients from an electrolytic strip analog were compared with the exact solution for the one-dimensional problem with leakage. No conclusive results were obtained from electrolytic analogs because of the limited amount of

data available. Several factors, especially discontinuities at the electrodes, still need considerable investigation.

The author feels that the validity of the conductive-paper analogs has been established and that a satisfactory method of determining the dimensionless time scales of such analogs has been demonstrated. These analogs should prove useful in the investigation of unsteady-flow fields of irregular shape.

LITERATURE CITED

1. Carslaw, H. S. and Jaeger, J. C. Conduction of heat in solids. 2nd ed. Oxford, England, Clarendon Press. 1959.
2. Churchill, R. V. Fourier series and boundary value problems. New York, N. Y., McGraw-Hill Book Co., Inc. 1941.
3. Clark, A. V. Simplified method for study of two-dimensional transient heat flow using resistance paper. Am. Soc. Mech. Engrs. Paper No. 57 S-9. 1957. (Original not available; abstracted in Mech. Engr. 79: 583. June 1957.)
4. Cohen, Louis. Heaviside's electrical circuit theory. New York, N. Y., McGraw-Hill Book Co., Inc. 1928.
5. Georgiev, A. M. The electrolytic capacitor. New York, N. Y., Technical Division, Murray Hill Books, Inc. 1945.
6. Jakob, Max. Heat transfer. Vol. 1. New York, N. Y., John Wiley and Sons, Inc. 1949.
7. Murphy, Glenn. Similitude in engineering. New York, N. Y., The Ronald Press Co. 1950.
8. Paschkis, V. Combined geometric and network analog computer for transient heat flow. Am. Soc. Mech. Engrs. Trans., J. Heat Transfer 81C: 144-8. May 1959.
9. _____ . Periodic heat flow in building walls determined by electrical analogy method. Am. Soc. Heat. Vent. Engrs. Trans. 48: 75-90. 1942.
10. _____ and Baker, H. D. A method for determining unsteady-state heat transfer by means of an electrical analogy. Am. Soc. Mech. Engrs. Trans. 64: 105-110. 1942.
11. Shippy, D. J. An electrical analogy of the potential distribution in two-dimensional unsteady-flow fields. Unpublished M. S. thesis. Ames, Iowa, Library, Iowa State University of Science and Technology. 1954.

12. Williamson, E. D. and Adams, L. H. Temperature distribution in solids during heating or cooling. Phys. Rev. (Series 2) 14: 99-114. August 1919.

ACKNOWLEDGMENTS

The author wishes to express his appreciation to the following: the Department of Nuclear Engineering for making available much of the equipment and supplies used; the University Electronics Shop for suggestions on the minimizing of equipment loading difficulties and for the use of electronic equipment; Aerovox Corporation for supplying anodized aluminum foil and for suggesting an appropriate electrolyte; and Dr. Glenn Murphy for suggestion of the research topic and for his helpful advice.

APPENDIX

Derivation of the Differential Equation for
Electric Potential within a Two-Dimensional,
Continuous-Medium, Resistance-Capacitance Analog

A portion of the cross section of a continuous-medium analog is illustrated in Fig. 19. The current density \underline{J}_1 flowing within layer (1) is related to the electric potential ϕ_1 by the expression

$$\underline{J}_1 = \frac{1}{\rho} \underline{E}_1 = \frac{1}{\rho} (-\nabla\phi_1 - \frac{\partial \underline{A}_1}{\partial t}),$$

where: ρ is the resistivity of (1),

∇ is the vector operator, "del", in x and y, and

\underline{A} is the magnetic vector potential.

It is assumed that $\partial \underline{A}_1 / \partial t$ is negligible with respect to $\nabla\phi_1$.

Hence,

$$\underline{J}_1 = -\frac{1}{\rho} \nabla\phi_1 .$$

Further, it is assumed that everywhere within (1) variations of ϕ_1 with the coordinate z are negligible with respect to ϕ_1 itself, i.e., $\phi_1 = \phi_1(x,y,t)$ only. Thus the x and y components of \underline{J}_1 may be expressed as

$$J_{x1} = J_{x1}(x,y,t) \text{ only and}$$

$$J_{y1} = J_{y1}(x,y,t) \text{ only.}$$

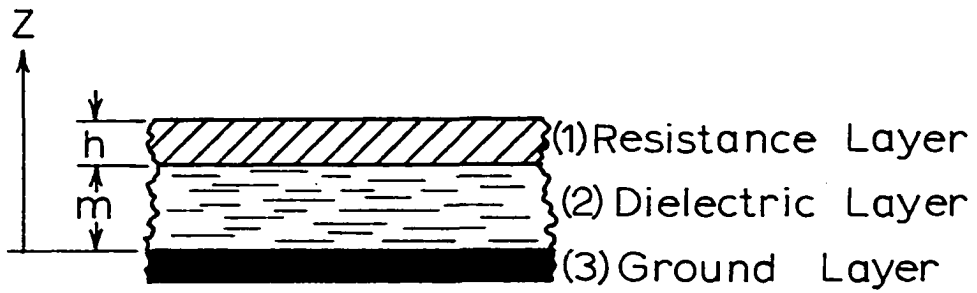


Fig. 19. Cross section of a continuous medium analog

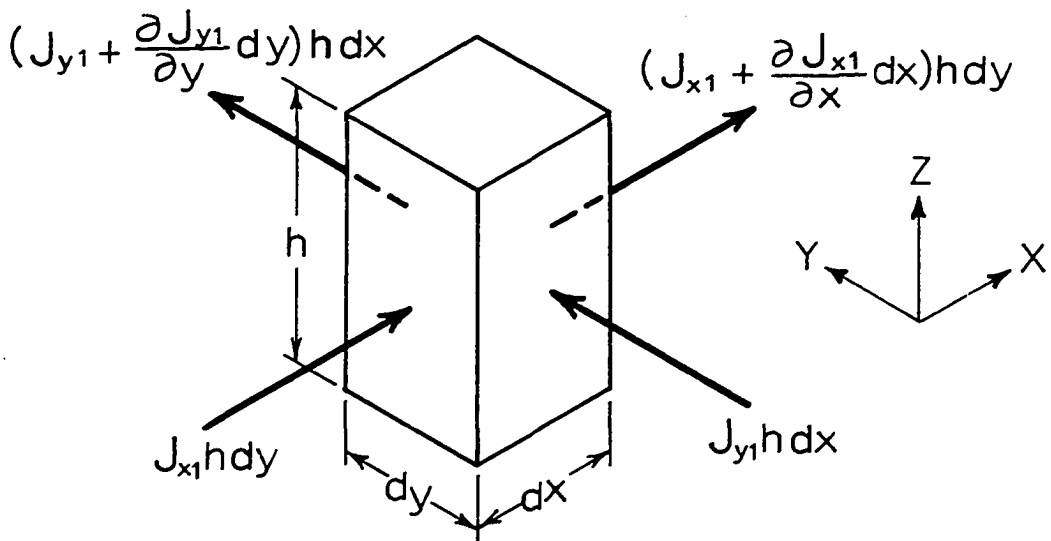


Fig. 20. Infinitesimal element of the resistance layer

Consider an infinitesimal element of (1) of area $dx dy$ and extending throughout the thickness h of (1), as in Fig. 20. As indicated in the diagram, currents enter and leave the lateral surfaces of the element. In addition, charge accumulates on the bottom surface of the element.

By conservation of charge (continuity) within the element,

$$-\left(\frac{\partial J_{x1}}{\partial x} dx\right)h dy - \left(\frac{\partial J_{y1}}{\partial y} dy\right)h dx = \frac{\partial \sigma_{12}}{\partial t} dx dy$$

where σ_{12} is the surface charge density at the surface of (1) in contact with (2). This expression may be written as

$$-h \frac{\partial J_{x1}}{\partial x} - h \frac{\partial J_{y1}}{\partial y} = \frac{\partial \sigma_{12}}{\partial t}$$

or

$$-h \frac{\partial \left(\frac{E_{x1}}{\rho}\right)}{\partial x} - h \frac{\partial \left(\frac{E_{y1}}{\rho}\right)}{\partial y} = \frac{\partial \sigma_{12}}{\partial t}$$

Assuming that ρ is constant throughout (1),

$$-\frac{h}{\rho} \frac{\partial E_{x1}}{\partial x} - \frac{h}{\rho} \frac{\partial E_{y1}}{\partial y} = \frac{\partial \sigma_{12}}{\partial t}$$

However, $\rho/h = \bar{R}'$, the resistance per square (x,y) of (1).

Thus

$$-\frac{\partial E_{x1}}{\partial x} - \frac{\partial E_{y1}}{\partial y} = \bar{R}' \frac{\partial \sigma_{12}}{\partial t}$$

or

$$\nabla^2 \phi_1 = \bar{R}' \frac{\partial \sigma_{12}}{\partial t}$$

At the (1-2) boundary,

$$(D_{z1})_2 - (D_{z2})_1 = \sigma_{12} ,$$

where $(D_{z1})_2$ is the z component of electric displacement in (1) at the boundary with (2). Similary, at the (2-3) boundary,

$$(D_{z2})_3 - (D_{z3})_2 = \sigma_{23}$$

However, it is assumed that layer (3) is composed of a perfect conductor and therefore $D_{z3} = 0$. Thus

$$(D_{z2})_3 = \sigma_{23}$$

It is assumed that the electric displacement in (2) may be expressed as

$$D_{z2} = D_{z2}(x,y,t) \text{ only.}$$

Hence

$$(D_{z2})_1 = (D_{z2})_3 = D_{z2} = \sigma_{23}$$

and

$$(D_{z1})_2 = \sigma_{23} + \sigma_{12}$$

By definition of electric permittivity ϵ , D_{z1} may be expressed as

$$D_{z1} = \epsilon_1 E_{z1} = \epsilon_1 (\rho J_{z1})$$

Therefore

$$\epsilon_1 \rho(J_{z1})_2 = \sigma_{23} + \sigma_{12}$$

It is assumed that

$$|\epsilon_1 \rho(J_{z1})_2| \ll |\sigma_{23}|.$$

Then

$$\sigma_{12} \approx -\sigma_{23}.$$

Also,

$$\sigma_{23} = D_{z2} = \epsilon_2 E_{z2} = \epsilon_2 \left(-\frac{\partial \phi_2}{\partial z}\right).$$

Integrating through layer (2),

$$\int_0^m \sigma_{23} dz = - \int_0^{\phi_1} \epsilon_2 d\phi_2.$$

Assuming that ϵ_2 is constant throughout (2),

$$\sigma_{23} m = -\epsilon_2 \phi_1.$$

Thus

$$\frac{\sigma_1}{\phi_{12}} = -\frac{\sigma_{23}}{\phi_{12}} = \frac{\epsilon_2}{m}$$

However, $\epsilon_2/m = \bar{\sigma}'$, the capacitance per unit area (x,y) of (2). Hence

$$\frac{\partial \sigma_1}{\partial t} = \bar{\sigma}' \frac{\partial \phi_1}{\partial t}.$$

Substitution of this last expression into the continuity equation results in

$$\nabla^2 \phi_1 = \bar{R}' \bar{C}' \frac{\partial \phi_1}{\partial t}$$

Check on the Validity of the Assumption that

$$\frac{\partial \underline{A}_1}{\partial t} \text{ is Negligible with Respect to } \nabla \phi_1$$

The assumption that $\frac{\partial \underline{A}_1}{\partial t}$ is negligible with respect to $\nabla \phi_1$ will be valid if the displacement current is negligible with respect to the conduction current. The criterion for the latter is that

$$\frac{1}{\rho^2 \epsilon_1^2 \omega^2} \gg 1$$

or

$$\omega^2 \ll \frac{1}{\rho^2 \epsilon_1^2}$$

where ω is the circular frequency.

For the conductive paper used in the present study,

$$\begin{aligned} h &= 0.004 \text{ inch} \approx (10^{-4}) \text{ meter} \\ \bar{R}' &= 1.79 (10^3) \text{ ohms} \approx 1.8 (10^3) \text{ ohms} \\ \epsilon_1 &\approx \epsilon_0 = 8.854 (10^{-12}) \text{ farad/meter} \\ &\approx 9 (10^{-12}) \text{ farad/meter.} \end{aligned}$$

Thus the resistivity is

$$\rho = h \bar{R}' \approx (10^{-4})(1.8)(10^3) = 0.18 \text{ ohm-meter}$$

and

$$\rho^2 \approx 0.032 \text{ ohm}^2\text{-meter}^2 .$$

Hence

$$\begin{aligned} \frac{1}{\rho^2 \epsilon_1^2} &\approx \frac{1}{0.032 [9(10^{-12})]^2} \\ &\approx 4(10^{23}) \text{ rad}^2/\text{sec}^2 \end{aligned}$$

Therefore if $\omega \ll 10^{12}$ rad/sec, the criterion will have been met and the original assumption will be valid.

Check on the Validity of the Assumption

$$\text{that } |\epsilon_1 \rho (J_{z1})_2| \ll |\sigma_{23}|$$

Consider the inequality

$$\int |\epsilon_1 \rho (J_{z1})_2| dx dy \ll \int |\sigma_{23}| dx dy$$

where $\int | \quad | dx dy$ indicates the definite integral over the entire surface of the analog. Since extreme variations of $(J_{z1})_2$ and σ_{23} with x and y are unlikely, the existence of the indicated inequality of the integrals would validate the assumption to be checked, i.e.,

$$|\epsilon_1 \rho (J_{z1})_2| \ll |\sigma_{23}| .$$

By continuity at the (1-2) interface,

$$(J_{z1})_2 = - \frac{\partial \sigma_{12}}{\partial t} .$$

Further, by the present assumption,

$$\sigma_{12} = -\sigma_{23} .$$

Therefore,

$$(J_{z1})_2 = \frac{\partial \sigma_{23}}{\partial t} .$$

Thus

$$\int |\epsilon_1 \rho (J_{z1})_2| dx dy = \epsilon_1 \rho \int \left| \frac{\partial \sigma_{23}}{\partial t} \right| dx dy = \epsilon_1 \rho \left| \frac{dQ_{23}}{dt} \right| = \epsilon_1 \rho |I|$$

where Q_{23} is the total charge at the (2-3) interface and hence I is the external current.

Also

$$\begin{aligned} \int |\sigma_{23}| dx dy &= \bar{C}' \int |\phi_{12}| dx dy = \bar{C}' s^2 \int |\phi_{12}| d\xi d\eta \\ &= \bar{C}' s^2 \phi_0 \int |\beta| d\xi d\eta \end{aligned}$$

where ϕ_0 is the input potential.

Thus, the inequality of the original integrals is equivalent to

$$\epsilon_1 \rho |I| \ll \bar{C}' s^2 \phi_0 \int |\beta| d\xi d\eta .$$

For a 10-inch-square paper analog,

$$\begin{aligned} \bar{C}' &\approx 5(10^{-4}) \text{ microfarad/square inch} \\ &\approx 8(10^{-7}) \text{ farad/meter}^2 \\ \epsilon_1 &\approx 9(10^{-12}) \text{ farad/meter} \end{aligned}$$

$$\rho \approx 0.18 \text{ ohm-meter}$$

$$s = 10 \text{ inches} \approx 0.25 \text{ meter}$$

The variation of $\int_0^1 \int_0^1 \beta d\xi d\eta$ with time, as computed from the exact solution, is indicated in Table 23. With an applied step input of $\phi_0 = 0.2$ volt, the measured variation of external current, I , with time is shown in Table 24. It can be seen from a comparison of Tables 23 and 24 that the critical time as far as the present assumption is concerned is immediately following the step change in input, i.e., at $\tau = 0^+$. At this instant, $|I| \approx 0.014$ ampere and $\int \beta d\xi d\eta \approx 1.00$. Using the above values,

$$\begin{aligned} \epsilon_1 \rho |I| &\approx 9(10^{-12})(0.18)(0.014) \\ &\approx 2(10^{-14}) \text{ coulomb} \end{aligned}$$

and

$$\begin{aligned} \bar{\sigma}' s^2 \phi_0 \int |\beta| d\xi d\eta &\approx 8(10^{-7})(0.25)^2(0.2)(1) \\ &\approx (10^{-8}) \text{ coulomb} \end{aligned}$$

Therefore, for the analog described, it is true that

$$\epsilon_1 \rho |I| \ll \bar{\sigma}' s^2 \phi_0 \int |\beta| d\xi d\eta$$

and the assumption is valid.

Table 23. Computed variation of $\int_0^1 \int_0^1 \rho d\xi d\eta$ with time for a square analog

Time, τ	$\int_0^1 \int_0^1 \rho d\xi d\eta$
0	1.000
0.05	0.559
0.10	0.413
0.20	0.246
0.30	0.150
0.50	0.056

Table 24. Measured variation of external current, I , with time for a 10-inch-square paper analog ($s = 10$ inches)

Time, τ	External current, I (10^{-3} amperes)
0	0
0+	13.6
0.05	0.6
0.10	0.4
0.50	0+

Check on the Validity of the Assumption that
Variations of ϕ_1 with z are Negligible
with Respect to ϕ_1

Because the top surface of layer (1) is an insulated boundary, at this surface

$$\frac{\partial \phi_1}{\partial z} = 0$$

and the maximum value of $\partial \phi_1 / \partial z$ will occur at the surface of (1) in contact with (2). Hence, the maximum variation of ϕ_1 with z in (1) must be less than $h(\partial \phi_1 / \partial z)_2$. Thus if

$$\left| h \left(\frac{\partial \phi_1}{\partial z} \right)_2 \right| \ll |\phi_1(x, y, t)|,$$

then variations of ϕ_1 and z will be negligible with respect to ϕ_1 , as assumed. Since extreme variations of $(\partial \phi_1 / \partial z)_2$ and ϕ_1 with x and y are unlikely, the existence of the above inequality would be established by showing that

$$h \int \left| \left(\frac{\partial \phi_1}{\partial z} \right)_2 \right| dx dy \ll \int |\phi_1| dx dy .$$

It is known that

$$\left(\frac{\partial \phi_1}{\partial z} \right)_2 = -(\mathcal{E}_{z1})_2 = -\rho (J_{z1})_2 = -\rho \frac{\partial \sigma_{23}}{\partial t}$$

and that

$$\int \frac{\partial \sigma_{23}}{\partial t} dx dy = I .$$

Therefore,

$$h \int \left| \left(\frac{\partial \phi_1}{\partial z} \right)_2 \right| dx dy = h\rho |I| .$$

It has also been shown that

$$\int |\phi_1| dx dy = s^2 \phi_0 \int |\beta| d\xi d\eta$$

Again, the critical time will be at $\tau = 0^+$. For the analog described previously,

$$|I| \approx 0.014 \text{ ampere}$$

and

$$\int |\beta| d\xi d\eta \approx 1.00 \text{ at } \tau = 0^+.$$

Then

$$\begin{aligned} h\rho |I| &\approx (10^{-4})(0.18)(0.014) \\ &\approx 3(10^{-7}) \text{ volt-meter}^2 \end{aligned}$$

and

$$\begin{aligned} s^2 \phi_0 \int |\beta| d\xi d\eta &\approx (0.25^2)(0.2)(1) \\ &\approx 10^{-2} \text{ volt-meter}^2 \end{aligned}$$

Consequently,

$$h\rho |I| \ll s^2 \phi_0 \int |\beta| d\xi d\eta$$

and the assumption is valid.